DOT/FAA/AR-07/2

Air Traffic Organization
Operations Planning
Office of Aviation Research
and Development
Washington, DC 20591

Thermal Analysis of Polymer Flammability

April 2007

Final Report

This document is available to the U.S. public through the National Technical Information Service (NTIS), Springfield, Virginia 22161.

U.S. Department of Transportation
Federal Aviation Administration

NOTICE

This document is disseminated under the sponsorship of the U.S. Department of Transportation in the interest of information exchange. The United States Government assumes no liability for the contents or use thereof. The United States Government does not endorse products or manufacturers. Trade or manufacturer's names appear herein solely because they are considered essential to the objective of this report. This document does not constitute FAA certification policy. Consult your local FAA aircraft certification office as to its use.

This report is available at the Federal Aviation Administration William J. Hughes Technical Center's Full-Text Technical Reports page: actlibrary.tc.faa.gov in Adobe Acrobat portable document format (PDF).

Technical Report Documentation Page

1. Report No.	2. Government Accession No.	3. Recipient's Catalog No.
DOT/FAA/AR-07/2		

4. Title and Subtitle	5. Report Date
THERMAL ANALYSIS OF POLYMER FLAMMABILITY	April 2007
	6. Performing Organization Code
7. Author(s)	8. Performing Organization Report No.
Richard E. Lyon, Robert Filipczak, Richard N. Walters*, Sean Crowley*, and Stanislav I. Stoliarov*	
9. Performing Organization Name and Address	
Federal Aviation Administration William J. Hughes Technical Center Airport and Aircraft Safety Research and Development Division Fire Safety Branch Atlantic City International Airport, NJ 08405 *SRA International 3120 Fire Road Egg Harbor Township, NJ 08234	
	11. Contract or Grant No.
12. Sponsoring Agency Name and Address	13. Type of Report and Period Covered
U.S. Department of Transportation Federal Aviation Administration Air Traffic Organization Operations Planning Office of Aviation Research and Development Washington, DC 20591	
	14. Sponsoring Agency Code ANM-110

15. Supplementary Notes

16. Abstract

A thermal analysis method is presented that uses controlled heating of polymer samples and complete combustion of the evolved gases to separately reproduce the condensed and gas phase processes of flaming combustion in a single laboratory test. Oxygen consumption calorimetry applied to the combustion gas stream gives the heat release rate history of the sample as a function of its temperature. The maximum rate of heat release and the temperature at which it occurs are polymer characteristics related to fire performance and flame resistance.

17. Key Words	18. Distribution Statement
Polymer, Plastic, Fire, Flammability, Flame, Heat release, Kinetics, Combustion, Oxygen consumption, Calorimetry	This document is available to the public through the National Technical Information Service (NTIS) Springfield, Virginia 22161

19. Security Classif. (of this report)	20. Security Classif. (of this page)	21. No. of Pages	22. Price
Unclassified	Unclassified	44	

Form DOT F 1700.7 (8-72) Reproduction of completed page authorized

ACKNOWLEDGEMENTS

The authors are indebted to Lauren Castelli and Qaadir Williams for the experimental values of heat release capacity. Although certain commercial equipment, instruments, materials, and companies are identified in this report in order to adequately specify the experimental procedure, this in no way implies endorsement or recommendation by the Federal Aviation Administration.

TABLE OF CONTENTS

		Page
EXECUTIVE SUMMARY		xi
1.	INTRODUCTION	1
2.	THEORY	1
2.1	Condensed Phase Model	1
2.2	Gas Phase Model	5
3.	EXPERIMENTAL	7
3.1	Materials	7
3.2	Methods	7
3.2.1	Thermogravimetry	7
3.2.2	Heat of Combustion	7
3.2.3	Thermal Oxidation of Fuel Gases	7
3.2.4	Pyrolsyis Combustion Flow Calorimetry	8
3.3	Flammability Testing	10
4.	RESULTS	10
4.1	Thermogravimetry (Anaerobic Conditions)	10
4.2	Thermal Oxidation Kinetics of Combustible Gases	12
4.3	Pyrolysis-Combustion Flow Calorimetry	15
4.4	Oxidative Pyrolysis-Combustion Flow Calorimetry	21
4.5	Correlation of PCFC Data With Flammability	23
4.5.1	Ignitability	23
4.5.2	Fire Response	23
4.5.3	Flame Resistance	26
5.	CONCLUSIONS	29
6.	REFERENCES	29

LIST OF FIGURES

Figure		Page
1	Plot of Equation 5 for $A = 5 \times 10^{11}\ S^{-1}$, $E_a = 190$ Kj/Mole (Solid Line) Compared to Experimental Data (Symbols) for PA66	2
2	Flow Diagram for Pyrolysis-Combustion Flow Calorimetry	8
3	Schematic Drawing of PCFC	9
4	Calculated (Equation 7) Versus Measured Peak Mass Loss Rates in TGA for PMMA, Polyethylene, and Phenolic Triazine at Heating Rates, β = 1, 3, 5, 10, 20, 30, 100, and 200 K/min	11
5	Decomposition Temperature $T_{max}(\beta)$ Versus Heating Rate β for PE, PT, and PMMA	11
6	Maximum Specific Mass Loss Rate Versus Heating Rate for PE, PMMA, and PT Polymers	12
7	Reaction Time Versus Temperature for 99.5% Combustion of Methane Gas and Polymer Pyrolysis Products Calculated From Oxidation Kinetic Parameters	14
8	Oxygen Concentration of a Stoichiometric (1:2) CH_4:) O_2 Mixture in Nitrogen Exiting the Combustor at the Indicated Temperature	14
9	Heat Release Rate Histories of Common Polymers in PCFC	15
10	Maximum Specific HRR Q_{max} Versus Heating Rate β in PCFC for 1-mg Samples of PE, PS, PA66, PMMA, PBT, PPO, PC, POM, and PT	16
11	Q_{max}/β Versus β for PE, HIPS, PMMA, POM, and FEP	17
12	Comparison of Individual and Average Heat Release Capacities From Three Different Laboratories for the 14 Polymers in Table 3	18
13	Comparison of Heat Release Capacities Obtained by PCFC at β = 260 K/min and TGA-GC/MS at β = 10 K/min	19
14	Peak Height Versus Peak Area Method of Calculating the Heat Release Capacity	20
15	Residual Mass and Heat of Combustion of Pyrolysis Gases Versus Temperature for Test of Polycarbonate in TGA at β = 20 K/min	21
16	Specific HRR of Polycarbonate Versus Time and Temperature Obtained by oPCFC	22

17 Peak HRR in Cone Calorimeter at 50 kW/m^2 External Flux Versus Heat Release Capacity in PCFC 25

18 Peak HRR in OSU Versus Heat Release Capacity in PCFC 26

19 UL 94 V Rating Versus Heat Release Capacity of Polymers 27

20 Limiting Oxygen Index Versus Heat Release Capacity of Polymers 28

LIST OF TABLES

Table		Page
1	Oxidation Kinetic Parameters Determined Experimentally and Obtained From the Literature for Methane Gas and Some Polymer Pyrolysis Products	13
2	Net Heats of Combustion of Noncharring Polymer Pyrolzates by PCFC Compared to Oxygen Bomb Calorimeter Values	15
3	Flammability Parameters η_c, h_c^0, μ, and T_p for PCFC	17
4	Net Heat of Combustion of Charring ($\mu \neq 0$) and Noncharring ($\mu = 0$) Polymers Obtained by Oxygen Bomb Calorimetry and Oxidative Pyrolysis-Combustion Flow Calorimetry (oPCFC)	22
5	Critical Heat Flux Calculated From T_{max} Compared to Values Measured in a Fire Calorimeter	23

LIST OF ACRONYMS

ABS	Acrylonitrile-butadiene-styrene
CHF	Critical heat flux
FAA	Federal Aviation Administration
FEP	Fluorinated ethylene-propylene
GC	Gas chromatograph
HDPE	High density polyethylene
HIPS	High-impact polystyrene
HOC	Heat of combustion
HRP	Heat release parameter
HRR	Heat release rate
LOI	Limiting oxygen index
MS	Mass spectrometer
NR	No vertical rating
OPCFC	Oxidative pyrolysis-combustion flow calorimetry
OSU	Ohio State University
PA66	Polyhexamethyleneadipamide
PBT	Polybutyleneterephthalate
PC	Polycarbonate
PCFC	Pyrolysis-combustion flow calorimetry
PE	Polyamide
PEI	Polyethermide
PET	Polyethleneterephthalate
PMMA	Polymethylmethacrylate
POM	Polyoxymethylene
PP	Polypropylene
PPO	Polyphenleneoxide
PPS	Polyphenylenesulfide
PS	Polystyrene
PT	Phenolictriazine
PVC	Polyvinylchloride
TGA	Thermogravimetric analyzer

EXECUTIVE SUMMARY

A method for measuring thermal combustion properties of polymers (plastics) is described. Controlled heating of milligram-sized samples and complete combustion of the evolved gases separately reproduce the condensed and gas phase processes of flaming combustion in a single, rapid laboratory test. Oxygen consumption calorimetry applied to the combustion gas stream gives the heat release rate of the sample as a function of its temperature. The thermal combustion properties determined from the test include the maximum rate of heat release, total amount of heat released, and the temperature at which the heat is released. The maximum rate of heat release divided by the heating rate in the test is a derived property called the heat release capacity. Heat release capacity is related to flame resistance and fire performance using a simple burning model that shows good agreement with experimental data.

1. INTRODUCTION.

A considerable amount of effort has been expended to relate laboratory thermal analyses to flammability [1-16]. The motivation for these studies is the desire for quantitative data to be used in materials evaluation and the convenience of testing milligram-sized samples under equilibrium conditions. Most thermal analyses of flammability attempt to relate a single quasi-equilibrium property, such as char yield, heat of combustion, or thermal decomposition temperature, to fire or flame test performance. Individually, these material properties have found limited success as descriptors of flammability, and their interrelationship in the context of fire behavior has remained obscure [17]. The primary obstacles in relating polymer properties to flame and fire test results are the highly coupled nature of the gas and condensed phase processes of flaming combustion (heat and mass transfer), physical changes of the solid during burning (melting, dripping, swelling, and char barrier formation), and combustion inhibition in the gas phase due to the presence (halogens) or absence (oxygen) of chemical species in the flame.

In this report, a test method is described that separately reproduces the condensed phase (pyrolysis) and gas phase (combustion) processes of flaming combustion in a single laboratory test. A simple model of polymer combustion is used to interpret the test results, and excellent agreement with the experimental data is observed. A physical basis for thermal analysis of polymer flammability is, thus, established and a material property is identified that is a good predictor of fire behavior and flame resistance [18-26].

2. THEORY.

2.1 CONDENSED PHASE MODEL.

The burning of a condensed phase material (e.g., a solid polymer) produces volatile fuel species and possibly a solid carbonaceous char or ash under anaerobic conditions [12 and 13]. The material at the burning surface is heated at a rate that is the product of the surface temperature gradient and the surface recession velocity and is typically on the order of a few degrees Kelvin per second [18 and 19]. The process of volatile fuel generation at the burning polymer surface is well described by a single-step, anaerobic thermal decomposition reaction [18, 19, and 27-34],

$$P \rightarrow F(\uparrow) + C \tag{1}$$

where species P, F, and C represent the polymer (P) and its fuel gases (F) and solid thermal decomposition products (C), respectively. It can be shown that if m_P, m_F, and m_C are the masses of P, F, and C, at time t, $m = m_P + m_C$ is the sensible mass, $m_0 = m_P + m_F + m_C$ is the initial mass, and $\mu = m_C/m_0$ is a constant, then the instantaneous rate of mass loss/fuel generation is

$$-\frac{d\,m}{d\,t} = k_p(m - \mu m_0) \tag{2}$$

In equation 2,

$$k_p = A\exp\left[-\frac{E_a}{RT}\right] \tag{3}$$

is the pyrolysis (reaction (1)) rate constant at temperature T in terms of the frequency factor A, the global activation energy for pyrolysis Ea, and the gas constant R. Although the heating rate varies with depth in a burning polymer, the heating rate at a particular depth (e.g., the surface) is relatively constant during steady burning [18 and 19]. A constant heating rate, $dT/dt = \beta$, transforms the independent variable from time to temperature in equation 2, which is then integrated to obtain the fraction of the initial mass (m_0) remaining at temperature T [18 and 19].

$$\frac{m(T)}{m_0} = \mu + (1-\mu)e^{-y} \tag{4}$$

The exponent of equation 4, $y = (ART^2 \exp[-E_a/RT])/(\beta(E_a+2RT))$, is a complex function of temperature. The specific mass loss rate at temperature T for a constant heating rate β is obtained from equations 2 and 4.

$$-\frac{1}{m_0}\frac{dm}{dt} = (1-\mu)k_p e^{-y} \tag{5}$$

Figure 1 shows the mass loss rate history of polyhexamethyleneadipamide (PA66) at heating rate β = 10 K/minute measured under anaerobic conditions in a thermogravimetric analyzer (TGA) (see section 3). Also plotted in figure 1 is the calculated mass loss history at 10 K/minute using equation 5 with $A = 5 \times 10^{11}\ s^{-1}$ and E_a = 190 kJ/mole determined for PA66 by nonisothermal gravimetric analysis [35]. A reasonably good fit of the experimental data to equation 5 is obtained for these kinetic parameters that are typical of polymers [36 and 37]. Peak height (equation 7) and peak width (equation 8) are indicated by the arrows in the figure.

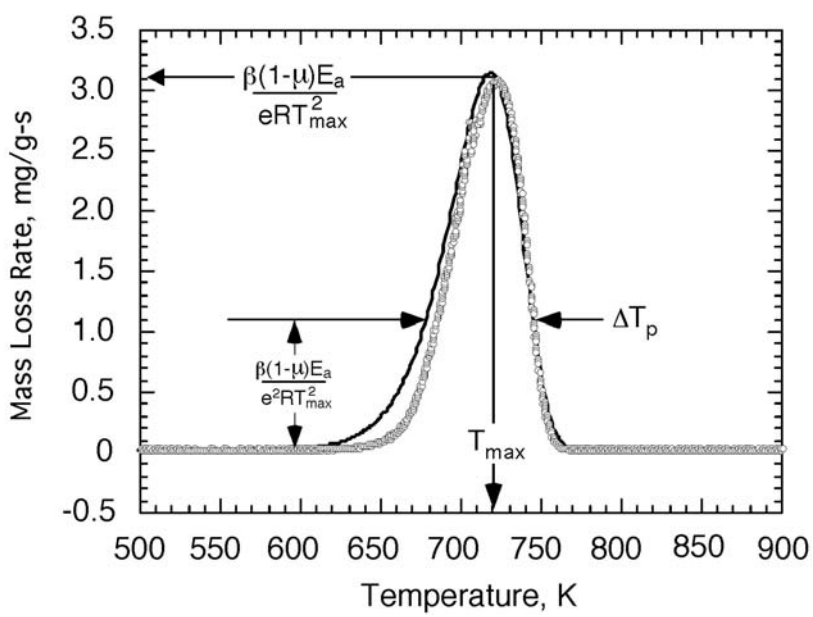

Figure 1. Plot of Equation 5 for $A = 5 \times 10^{11}\ S^{-1}$, E_a = 190 Kj/Mole (Solid Line) Compared to Experimental Data (Symbols) for PA66

An explicit result for the maximum specific mass loss rate in a constant heating rate experiment, such as that shown in figure 1, is found by setting the time derivative of equation 5 (or the second derivative of equation 4) equal to zero. The nontrivial ($\mu \neq 1$) result for the value of the rate constant at the peak mass loss rate temperature T_{max} is

$$k_p(\max) = \frac{\beta E_a}{RT_{max}^2} \tag{6}$$

Substituting k_p(max)/equation 6 into equation 5 gives the maximum specific mass loss rate of a sample that is uniform in temperature and is heated at a constant rate of temperature rise β [18 and 19],

$$\left.\frac{-1}{m_0}\frac{d\,m}{d\,t}\right|_{max} = \frac{\beta(1-\mu)E_a}{e^{\gamma}RT_{max}^2} \approx \frac{\beta(1-\mu)E_a}{eRT_{max}^2} \tag{7}$$

where, $\gamma = E_a/(E_a + 2RT_{max}) \approx 1$ for typical $E_a >> RT_{max}$. The maximum fractional mass loss rate of PA66 measured experimentally is 3.1 mg/g-s (see figure 1) compared to 2.9 mg/g-s calculated from equation 7 for kinetic parameters, E_a = 190 kJ/mole, μ = 0, and T_{max} = 720 K. A characteristic temperature interval for pyrolysis can be defined as

$$\Delta T_p \equiv \frac{-\frac{1}{m_0}\int_{T_0}^{T_\infty}\frac{dm}{dt}dT}{\left.-\frac{1}{m_0}\frac{dm}{d\,t}\right|_{max}} = \frac{-\beta\frac{1}{m_0}\int_0^{\infty}\frac{dm}{dt}dt}{\beta(1-\mu)E_a/eRT_{max}^2} = \frac{\beta(1-\mu)}{\beta(1-\mu)E_a/eRT_{max}^2} = \frac{eRT_{max}^2}{E_a} \tag{8}$$

Evaluating equation 5 at $T = T_{max} \pm \Delta T_p/2 = T_{max} \pm eR\,T_{max}^2/2E_a$ shows that, on average, the mass loss rate falls to 1/e of the maximum value at $\Delta T_p = eR\,T_{max}^2/E_a$ for typical [36 and 37] polymer E_a, T_{max}, i.e.,

$$\left.\frac{-1}{m_0}\frac{d\,m}{d\,t}\right|_{T=T_{max}\pm\frac{\Delta T_p}{2}} \approx \frac{1}{e}\left(\left.\frac{-1}{m_0}\frac{d\,m}{d\,t}\right|_{max}\right) = \frac{\beta(1-\mu)E_a}{e^2RT_{max}^2} \tag{9}$$

The temperature at maximum mass loss rate T_{max} and the pyrolysis interval $\Delta T_p = eR\,T_{max}^2/E_a$ is also plotted in figure 1.

The heating rate dependence of T_{max} is obtained by setting equations 3 and 6 equal at $T = T_{max}$ during a constant heating rate experiment.

$$\frac{\beta E_a}{ART_{max}^2}\exp\left[\frac{E_a}{RT_{max}}\right] = 1 \tag{10}$$

The frequency factor A can be eliminated from equation 10 by defining a reference heating rate β_0 for which $T_{max}(\beta_0) = T_{max,0}$.

$$\frac{\beta E_a}{ART_{max}^2}\exp\left[\frac{E_a}{RT_{max}}\right] = \frac{\beta_0 E_a}{ART_{max,0}^2}\exp\left[\frac{E_a}{RT_{max,0}}\right] = 1 \tag{11}$$

The temperature at maximum specific mass loss rate $T_{max}(\beta) = T_{max}$ at heating rate β is obtained from equation 11 as

$$\frac{1}{T_{max}} = \frac{1}{T_{max,0}} + \frac{R}{E_a}\ln\left[\frac{\beta_0}{\beta}\right] - \frac{R}{E_a}\ln\left[\frac{T_{max,0}}{T_{max}}\right]^2 \tag{12}$$

Changes in T_{max} are small relative to changes in β for typical [36 and 37] polymer activation energies $E_a \approx 200 \pm 50$ kJ/mole and decomposition temperatures [36-38] $T_{max} \approx 700 \pm 50$K, so the last term on the right-hand side of equation 12 can be neglected, and

$$\frac{1}{T_{max}} \approx \frac{1}{T_{max,0}} + \frac{R}{E_a}\ln\left[\frac{\beta_0}{\beta}\right] \tag{13}$$

Substituting equation 13 into equation 7 gives an explicit result for the maximum mass loss rate in a constant heating rate experiment in terms of the kinetic parameters

$$\left.\frac{-1}{m_0}\frac{d\,m}{d\,t}\right|_{max} = \frac{\beta(1-\mu)E_a}{eRT_{p,0}^2}\left\{1 + \frac{2RT_{max,0}}{E_a}\ln\left[\frac{\beta_0}{\beta}\right] + \left(\frac{RT_{max,0}}{E_a}\ln\left[\frac{\beta_0}{\beta}\right]\right)^2\right\} \tag{14}$$

Defining $x \equiv \beta_0/\beta$ and $a \equiv 2RT_{max,0}/E_a$ and substituting these into equation 14 shows that the bracketed quantity resembles the series expansion for an exponential

$$x^a = 1 + a\,ln[x] + (a\,ln[x])^2/2! + (a\,ln[x])^3/3! + \cdots$$

For common polymers [36-38] under typical [39 and 40] experimental conditions of thermogravimetry, $a = 2RT_{max,0}/E_a \approx (2)(8.314\text{ J/mole-K})(700 \pm 50\text{K})/(200 \pm 50\text{ kJ/mole}) = 0.06 \pm 0.01$. Hence, $a << 1$ and since $ln[x] = ln[\beta_0/\beta]$ is of unit order for the decade range of heating rates encountered in thermogravimetric analyses (and fires), both x^a and the bracketed quantity in equation 14 can be approximated with a sufficient accuracy by the first two terms of the series, which allows to simplify the heating rate dependence of the maximum specific mass loss rate.

$$\left.\frac{-1}{m_0}\frac{d\,m}{d\,t}\right|_{max} = \frac{\beta(1-\mu)E_a}{eRT_{max}^2} = \frac{\beta_0(1-\mu)E_a}{eRT_{max,0}^2}\left[\frac{\beta}{\beta_0}\right]^{1-a} = \left.\frac{-1}{m_0}\frac{d\,m}{d\,t}\right|_{max,0}\left[\frac{\beta}{\beta_0}\right]^{1-a} \tag{15}$$

Multiplying equation 15 by the heat of complete combustion of the pyrolysis products $h_{c,v}^0$ gives the maximum specific heat release rate (HRR) (W/kg) of a polymer sample whose temperature is uniform and increases at a constant rate during which all of the pyrolysis gases are completely and instantaneously combusted.

$$Q_{max}(\beta) = \frac{-h^0_{c,v}}{m_0}\frac{d\,m}{d\,t}\bigg|_{max} = \frac{-h^0_{c,v}}{m_0}\frac{d\,m}{d\,t}\bigg|_{max,0}\left[\frac{\beta}{\beta_0}\right]^{1-a} = Q_{max}(\beta_0)\left[\frac{\beta}{\beta_0}\right]^{1-a} \tag{16}$$

Dividing the maximum specific HRR Q_{max} (equation 16) by β yields

$$\frac{Q_{max}(\beta)}{\beta} = \frac{Q_{max}(\beta_0)}{\beta_0}\left(\frac{\beta_0}{\beta}\right)^a = \eta_c\left(\frac{\beta_0}{\beta}\right)^a \tag{17a}$$

or

$$\eta_c = \frac{h^0_{c,v}(1-\mu)E_a}{eRT^2_{max,0}} = \frac{Q_{max}}{\beta}\left[\frac{\beta}{\beta_0}\right]^a \tag{17b}$$

Substituting equation 8 into equation 17b

$$\eta_c = \frac{h^0_c}{\Delta T_{p,0}} = \frac{Q_{max}}{\beta}\left[\frac{\beta}{\beta_0}\right]^a \tag{18}$$

Equation 18 shows that η_c is the average amount of heat released by combustion of the pyrolysis gases per degree of temperature rise over the pyrolysis interval. η_c is defined at a specific heating rate (β_0). However, it can be calculated from the data obtained at a different heating rate (β) using equation 18. η_c has the units and significance of a heat (release) capacity [18-23]. For a polymer that decomposes by a first order (single step) process, the heat release capacity η_c is seen to be a particular function of thermal stability (E_a, T_{max}) and combustion (μ, $h^0_{c,v}$) properties, each of which is known to be separately calculable from additive molar group contributions [37, 38, and 41]. Consequently, η_c should be (and is) calculable from additive molar group contributions [23].

2.2 GAS PHASE MODEL.

The reaction of volatile fuel F (e.g., equation 1) with oxygen typically yields complete (CO_2, H_2O, HX) and incomplete (CO, HC) combustion products, where X is a halogen, HX is a halogen acid, and HC is a solid or gaseous hydrocarbon.

$$F + gO_2 \rightarrow aCO_2 + bCO + cH_2O + hHX + eHC \tag{19}$$

Rarely is the stoichiometric oxygen/fuel ratio known in advance, and combustion is never 100% complete during the burning of polymers because of kinetic and diffusion limitations in the gas phase. In equation 19, g = a + b/2 + c/2, and the rate of fuel consumption by oxidation (assuming the second order kinetics) is

$$-\frac{d[F]}{d\,t} = k_c[F][O_2] \tag{20}$$

where [F] and $[O_2]$ are the molar concentrations of fuel and oxygen, respectively, in the gas phase, and k_c is the global rate constant for combustion. For combustion in a large excess of oxygen where $[O_2] \approx [O_2]_0$ is approximately constant, equation 20 becomes

$$-\frac{d[F]}{dt} = \{k_c[O_2]_0\}[F] = k_{app}[F] \tag{21}$$

$k_{app} = [O_2]_0 k_c$ is an apparent rate constant for fuel combustion. Equation 21 is solved immediately for the isothermal fuel concentration at time t.

$$\frac{[F]}{[F]_0} = 1 - \chi = e^{-k_{app}t} \tag{22}$$

Where $\chi = \chi(t,T)$ is the extent of reaction expressed as the change in fuel concentration $\Delta[F]$ at elapsed time t, temperature T, divided by the change in fuel concentration for complete reaction $\Delta[F]_0$. The relationship between χ and the oxygen consumed by combustion follows directly from equation 19.

$$\chi = \chi(t,T) = \frac{\Delta[F]}{\Delta[F]_0} = \frac{g\Delta[O_2]}{g\Delta[O_2]_0} = \frac{\Delta[O_2](t,T)}{\Delta[O_2](\max)} \tag{23}$$

If oxygen is present in large excess and there is sufficient time and temperature for complete combustion, then $\chi = 1$, [F] = 0 and fuel F is quantitatively converted to CO_2, H_2O, and possibly HX. For complete combustion, the amount of oxygen consumed is uniquely related to the fuel composition, $F = C_cH_hO_mN_nX_x$,

$$C_cH_hO_mN_nX_x, + (c + \frac{h-x-2m}{4})\, O_2 \rightarrow cCO_2 + \frac{h-x}{2}\, H_2O + \frac{n}{2}N_2 + xHX \tag{24}$$

The stoichiometric oxygen/fuel mass ratio r_0 is readily calculated from equation 24 for fuels of known composition and is in the range $r_0 = 2.0 \pm 1.5$ for the majority of organic compounds [42]. Thornton [43] was the first to notice that the heat of combustion of organic gases and liquids h_c^0 (J/g-fuel) divided by the stoichiometric mass ratio was essentially constant and independent of the type of fuel

$$C = h_c^0/r_0 = 13.1 \pm 0.7 \text{ MJ/kg-}O_2 \tag{25}$$

This observation was extended to solids by Huggett [44] and became the basis for oxygen consumption calorimetry [45 and 46], whereby measurement of the mass of oxygen consumed from the combustion atmosphere is used to deduce the amount of heat released during the burning of materials and products [47 and 48]. Equation 25 is valid only for complete combustion, i.e., equation 24.

3. EXPERIMENTAL.

3.1 MATERIALS.

Thermoplastic and thermoset polymers tested in the laboratory were unfilled, natural, or virgin resins obtained from Aldrich Chemical Company, Scientific Polymer Products, original manufacturers, and plastics suppliers. Thermoset polymer composites were fabricated in the laboratory as single or multiple layers of glass or carbon fiber fabrics impregnated with resin by hand lay-up, or resin transfer molding, and cured to completion. Methane, oxygen, and nitrogen gases used for calibration and testing were dry, ultra-high purity (> 99.5%) grades obtained from Matheson Gas Products.

3.2 METHODS.

3.2.1 Thermogravimetry.

Thermogravimetric analyses were performed at various heating rates, but typically at $\beta = 10$ K/min under nitrogen flow of 80 cm^3/min in commercial instruments (STA-851e, Mettler Toledo or TGA-7, Perkin Elmer), using a standard method [40]. Sample mass was between 1 and 5 mg in all cases.

3.2.2 Heat of Combustion.

Net heats of complete combustion of solid polymers [41, 42, and 49] were determined on 1-gram samples tested in triplicate using high-pressure oxygen bomb calorimetry according to a standard method [50]. The net heat of combustion was determined from the gross calorific value by subtracting the heat of vaporization of water for these polymers of known composition.

3.2.3 Thermal Oxidation of Fuel Gases.

Thermal oxidation kinetics of fuel gases were studied to determine the time-temperature requirements for complete combustion of polymer pyrolysis products under laboratory conditions. In these experiments, methane and polymer (polymethylmethacrylate (PMMA), polypropylene (PP)) pyrolyzates were mixed with twice the amount of oxygen required for complete oxidation to carbon dioxide and water, e.g., equation 19 with $b = h = e = 0$. The apparatus used for the oxidation kinetic experiments has been described previously [45 and 46] and consists of a pyrolysis probe (Pyroprobe 2000, CDS Analytical) in a heated manifold attached to a 5-m-long Inconel combustion tube having an inner diameter of 4.5 mm, which is coiled to fit inside a ceramic furnace. The oxygen/fuel mass ratio r was held constant at $r \geq 2r_0$ so that oxygen was always present in excess while the residence time of the gases and the temperature of the combustor were independently varied in stepwise increments of 50 cm^3/min between flow rates of 50-200 cm^3/min and in 10°C increments between combustor temperatures of 500°-1000°C. The oxidized gas stream was analyzed for residual oxygen to compute the extent of reaction χ as per equation 23 for a particular time and temperature in the combustor. Fuel gases tested were methane (4% by volume in air), the volatile pyrolysis products of PMMA (which depolymerizes to methylmethacrylate monomer), and the pyrolysis products of polypropylene (which thermally degrades by random and beta scission to alkanes and alkenes).

Equation 22 was used to model the isothermal oxidation kinetics as a single-step process with apparent rate constant

$$k_{app} = [O_2]_0 A_c \exp\left[-\frac{E_c}{RT}\right] \tag{26}$$

where A_c (m^3/(mol-s)) is the pre-exponential factor and E_c (kJ/mol) is the activation energy for the fuel-oxygen reaction, and $[O_2]_0$ = 8.6 mol/m^3 is the oxygen concentration used in the experiments. According to equations 22-24, the slope of a plot of $-ln[1-\chi]$ versus time t at constant temperature T is the apparent rate constant $k_{app}(T)$. The oxidation kinetic parameters E_c and A_c can then be determined from the slope and intercept, respectively, of a plot of $ln[k_{app}(T)]$ versus 1/T as per equation 26 written in logarithmic form

$$ln\{k_{app}(T)/ [O_2]_0\} = lnA_c - (E_c/R)(1/T) \tag{27}$$

3.2.4 Pyrolysis Combustion Flow Calimetry.

Thermal analysis of polymer flammability was conducted using pyrolysis combustion flow calorimetry/PCFC [51-55]. The PCFC methodology, shown schematically in figure 2, uses oxygen consumption calorimetry [45 and 46] to measure the rate and amount of heat produced by complete combustion of the fuel gases generated during controlled pyrolysis of milligram-sized samples. The method is implemented as a stand-alone device, as shown in figure 3, or as an evolved gas accessory attached to a TGA. In the stand-alone apparatus, 1-5-milligram samples are heated to 800°C at a heating rate of 1°C/s (typically) in a stream of nitrogen flowing at 80 cm^3/min. The volatile thermal degradation products are swept from the pyrolyzer by the nitrogen purge gas and mixed with 20 cm^3/min of pure oxygen prior to entering the combustor, held at 900°C (see section 4.2). After exiting the combustor, the gas stream passes over anhydrous calcium sulfate (Drierite) to remove moisture and acid gases prior to passing through a mass flow meter and oxygen analyzer to calculate the HRR by oxygen consumption.

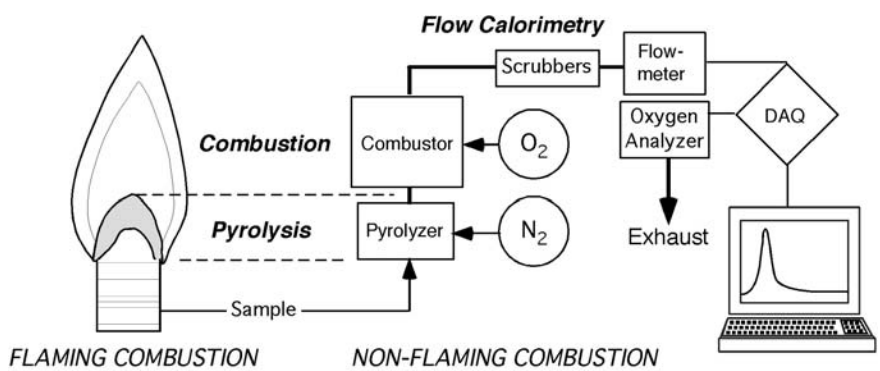

Figure 2. Flow Diagram for Pyrolysis-Combustion Flow Calorimetry

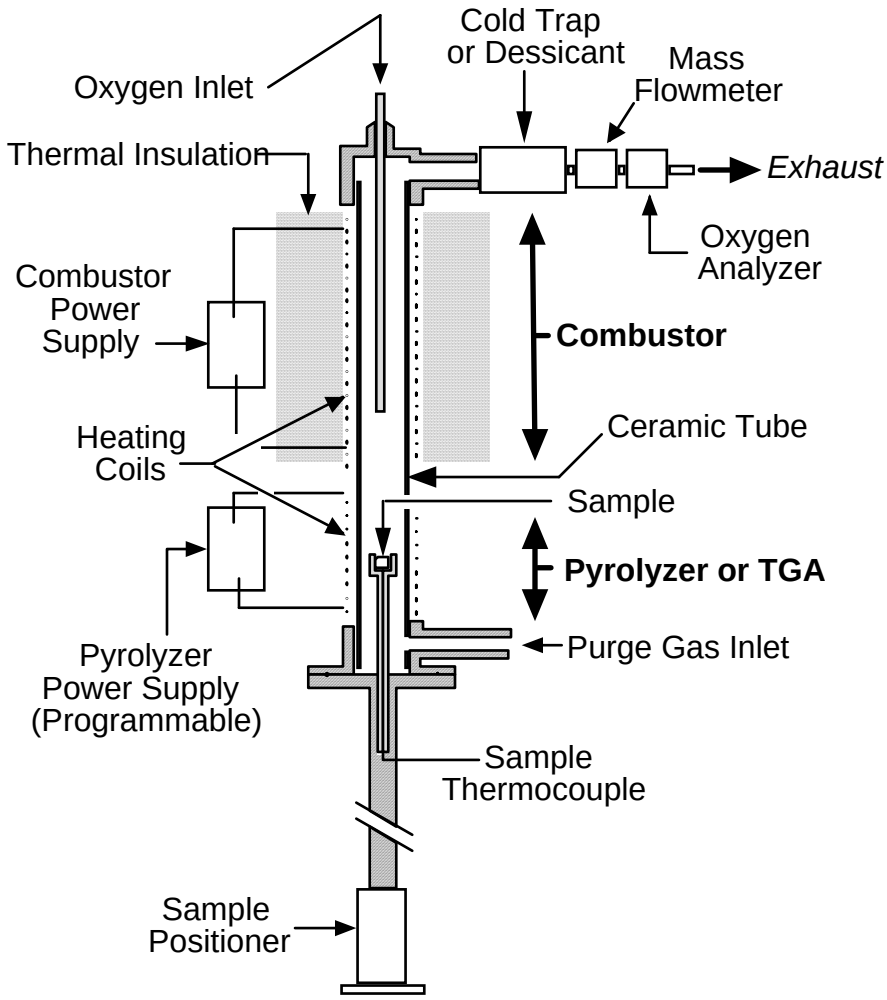

Figure 3. Schematic Drawing of PCFC

Experiments were also conducted in which the combustor was attached to the furnace of a TGA (STA-851e, Mettler-Toledo) to thermally oxidize the evolved pyrolysis gases. Three to five samples of each polymer were tested. The HRR data were synchronized with the sample temperature by subtracting the transit time of the gases from the pyrolyzer (PCFC) or TGA furnace (STA) to the oxygen analyzer.

Experiments were also conducted in which the purge gas was air rather than nitrogen to effect oxidative pyrolysis. In these experiments, both the sample gases and the solid pyrolysis residue/char are completely oxidized and the net heat of combustion of the entire sample is measured by oxygen consumption.

Experiments were also conducted in which the purge gas was methane (8.3 cm^3/min) and nitrogen (75 cm^3/min) and the oxygen flow rate was 16.7 cm^3/min, so that the molar ratio of oxygen/fuel was stoichiometric, i.e., $[O_2]/[CH_4] = 2$. The combustor temperature was slowly cycled between 25° and 950°C so that the temperature of the $CH_4/O_2/N_2$ gas mixture did not change significantly during the 10-second residence time in the combustor. The oxidized gas

stream was analyzed for residual oxygen to compute the extent of reaction as a function of combustor temperature for a residence time of 10 seconds.

3.3 FLAMMABILITY TESTING.

Fire calorimetry tests were conducted in a cone calorimeter (Cone2 Combustion Analysis System, Atlas Fire Science Products and Cone Calorimeter, Fire Testing Technologies) according to standard methods [47] on polymer and polymer composite samples having dimensions 100 x 100 x 6 mm. Fire calorimetry tests were also conducted in the Ohio State University (OSU) calorimeter according to the Federal Aviation Administration (FAA) protocol for flammability testing of commercial aircraft cabin interior materials [56]. Thermoplastic samples for OSU tests were 150 x 150 x 1.6 mm, while thermoset resins were tested as composite lamina (single layers) reinforced with fiberglass or carbon fabric and having a typical thickness of 0.3 mm. Flame resistance was measured according to standard methods [57 and 58]. Fire calorimetry data and flame resistance data were also obtained from product literature, scientific journals, and handbooks as generic values.

The specific HR rate is calculated from equations 16 and 25 for an initial sample mass m_0, in terms of the instantaneous change in the mass fraction of oxygen in the dried combustion gas stream Δm_{O_2}, the dry gas stream density ρ (kg/m^3), and the volumetric flow rate F (m^3/s),

$$Q(t) = \frac{-h^0_{c,v}}{m_0}\frac{d\,m}{d\,t} = \frac{C}{m_0}\frac{d\,r_0 m}{d\,t} = \frac{\rho C F}{m_0}\Delta m_{O_2}(t) \tag{28}$$

where C = 13.1 ±0.6 MJ/kg-O_2 is essentially the heat of combustion of oxygen with typical organic fuels. The heat of combustion of the fuel gases per unit initial mass of sample h^0_c (J/g) = $(1-\mu)\,h^0_{c,v}$ is obtained directly by time-integration of Q(t) over the entire test, i.e.,

$$h^0_c \equiv (1-\mu)h^0_{c,v} = \int_0^\infty Q(t)dt = \frac{C}{m_0}\int_0^\infty \rho F \Delta m_{O_2}(t)dt \tag{29}$$

The char fraction μ is obtained by weighing the sample before and after the test. The heat release capacity η_c (J/g-K) is obtained by dividing the maximum value of the specific HRR Q_{max} by the heating rate in the test β.

4. RESULTS.

4.1 THERMOGRAVIMETRY (ANAEROBIC CONDITIONS).

Figure 4 shows experimental data [27] for the maximum specific mass loss rate of PMMA (E_a = 160 kJ/mol, μ = 0), polyethylene/PE (E_a = 264 kJ/mol, μ = 0), and phenolic triazine/PT (E_a = 178 kJ/mol, μ = 0.7) versus heating rate in nitrogen compared to values calculated using equation 7 with $T_{max}(\beta)$ measured during the test. Close proximity of the calculated and measured peak mass loss rates to the equivalence line on the log-log plot indicates that equation 7 is valid over several decades of heating rate in the vicinity of fire heating rates (1-10 K/s) if the temperature at

maximum mass loss rate $T_{max}(\beta)$ is used in the calculation with the activation energy and char yield for the polymer determined in separate experiments.

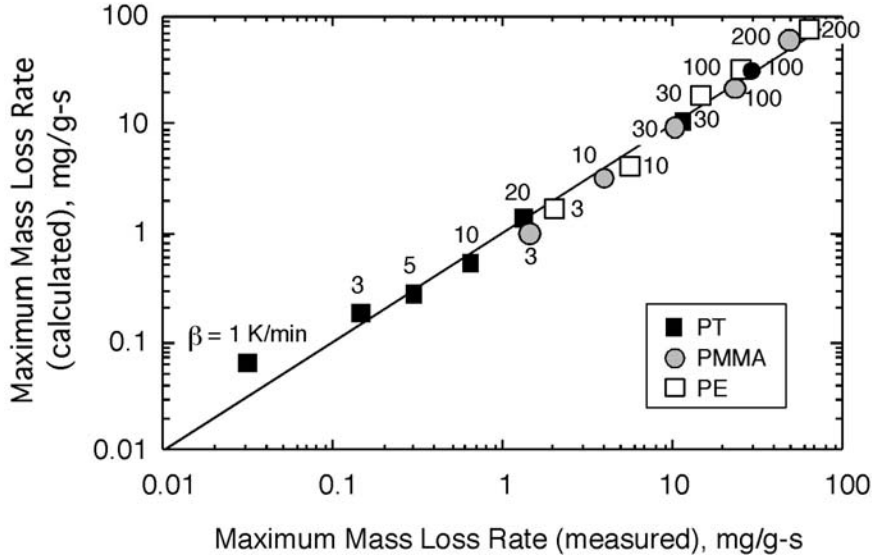

Figure 4. Calculated (Equation 7) Versus Measured Peak Mass Loss Rates in TGA for PMMA, Polyethylene, and Phenolic Triazine at Heating Rates, β = 1, 3, 5, 10, 20, 30, 100, and 200 K/min

Figure 5 shows T_{max} versus heating rate data [27] for high-density polyethylene (HDPE), phenolictriazine (PT), and PMMA as filled and open circles. Solid lines through the experimental data in figure 5 were calculated using equation 13 with β_0 = 10 K/min and activation energies obtained by nonisothermal methods [27 and 35], E_a = 264 kJ/mol, 178 kJ/mol, and 160 kJ/mol for PE, PT, and PMMA, respectively. The corresponding char yields and peak decomposition temperatures are μ = 0, 0.7, 0, and $T_{max,0}$ = 757K, 735K, and 653K for HDPE, PT, and PMMA, respectively.

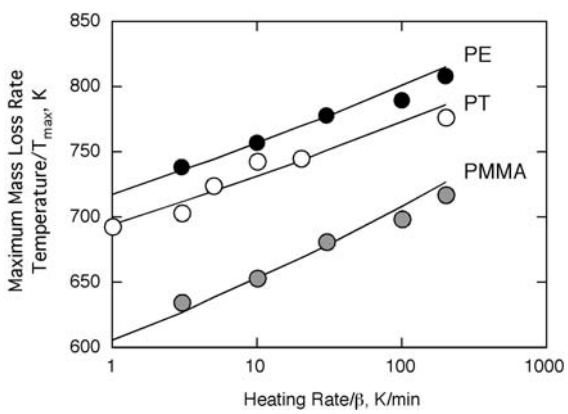

Figure 5. Decomposition Temperature $T_{max}(\beta)$ Versus Heating Rate β for PE, PT, and PMMA (Circles are Experimental Data. Lines are Equation 13 With Reported E_a and β_0 = 10 K/min.)

Figure 6 is a plot of the maximum specific mass loss rate versus heating rate for PE, PT, and PMMA obtained by TGA under nitrogen purge. Symbols are experimental data. Solid lines were calculated using equation 15 for a reference heating rate $\beta_0 = 10$ K/min.

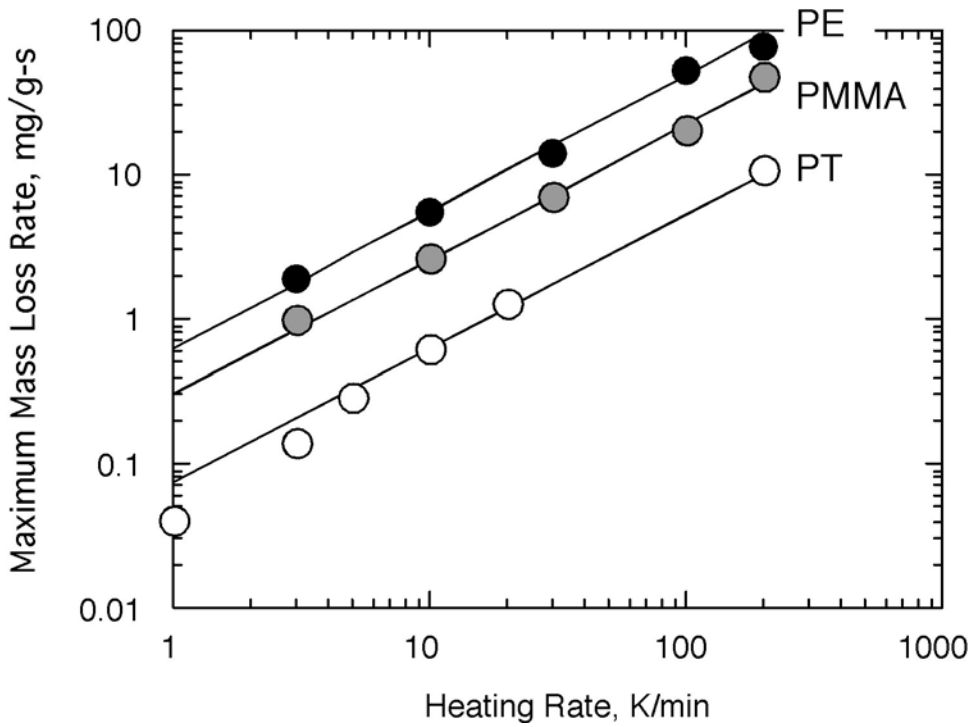

Figure 6. Maximum Specific Mass Loss Rate Versus Heating Rate for PE, PMMA, and PT Polymers (Circles are Experimental Data. Lines are Equation 15 With $\beta_0 = 10$ K/min.)

4.2 THERMAL OXIDATION KINETICS OF COMBUSTIBLE GASES.

Experimental results for $A = A_c[O_2]_0$ and E_c from thermal oxidation studies of methane (methane 1) and the pyrolyzates of PMMA and polypropylene (PP), are listed in table 1. Also listed in table 1 are values of A and E_c obtained from the literature for methane (methane 2) [59] as well as the pyrolysis products of some common hydrocarbon polymers [60].

Table 1. Oxidation Kinetic Parameters Determined Experimentally and Obtained From the Literature [59 and 60] for Methane Gas and Some Polymer Pyrolysis Products

Polymer	E_c (kJ/mole)	A (s^{-1})	Temperature Range (K)	Reference
Methane gas (methane 1)	241	10^{12}	1020-970	-
Methane gas (methane 2)	230	10^{10}	1000-2000	59
PMMA 1	62	10^{4}	725-973	60
PMMA 2	130	10^{7}	773-898	-
Polypropylene	94	10^{5}	607-656	-
Polybutadiene	91	10^{5}	800-945	60
Polyisoprene	75	10^{4}	825-975	60
Ethylene-propylene rubber	133	10^{8}	800-975	60
PC/ABS blend	188	10^{10}	800-975	55

From equations 22 and 25 and the data in table 1, the minimum residence time in the combustor at temperature T_c for any degree of oxidation can be calculated. If the oxidation reaction of the fuel gases in the presence of excess oxygen is required to be 99.5% complete by the time the gas stream exits the combustor, then the minimum residence time τ_r in the combustor at temperature T_c is

$$\tau_r = \frac{-\ln(1-0.995)}{A\exp[-E_c/RT_c]} = \frac{5.3}{A\exp[-E_c/RT_c]} \tag{30}$$

Equation 30 is plotted in figure 7 as reaction time τ_r versus temperature for the materials and kinetic parameters in table 1. Figure 7 shows that for all the fuels examined, thermal oxidation is 99.5% complete in 1 second at 1000°C, or in 10 seconds at 900°C, without the use of a catalyst. These results are significantly different from the 50 seconds at 1000°C claimed by Babrauskas, et al. [61] to be necessary for complete thermal oxidation of fire gases containing soot particles using a platinum catalyst.

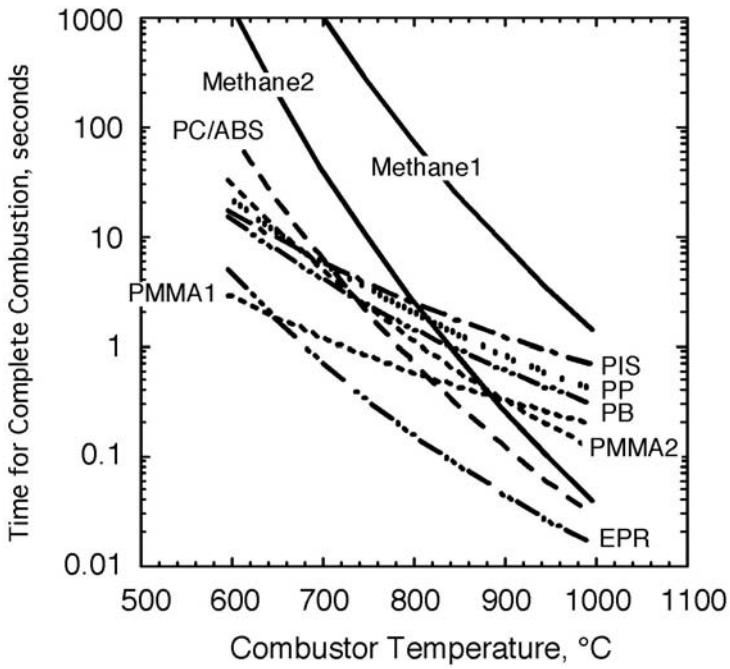

Figure 7. Reaction Time Versus Temperature for 99.5% Combustion of Methane Gas and Polymer Pyrolysis Products Calculated From Oxidation Kinetic Parameters

The results of combustor temperature cycling experiments for the stoichiometric mixture of methane and oxygen in nitrogen are shown in figure 8 as the final oxygen concentration of the combustion stream versus the combustor temperature over the range 500°-900°C. It is apparent that the oxygen concentration goes to zero, i.e., all the oxygen (and methane) is consumed during the 10-second residence time in the combustor at temperatures between 775° and 800°C. This result is in general agreement with the data in figure 7 with the exception of methane1. The absence of any residual oxygen in the stoichiometric reaction with methane shows that oxygen is not rate limiting under the conditions of these experiments. The hysteresis in the $[O_2]$ versus time data is due to thermal lag of the temperature measurement.

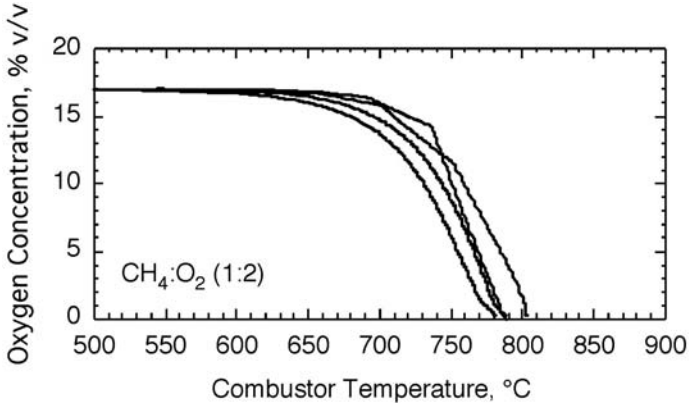

Figure 8. Oxygen Concentration of a Stoichiometric (1:2) CH_4:O_2 Mixture in Nitrogen Exiting the Combustor at the Indicated Temperature

Table 2 lists the heats of combustion of the pyrolysis products (monomers and oligomers) of noncharring polymers measured in the PCFC for a residence time of 10 seconds at 900°C in the combustor. Also listed in table 2 are heats of complete combustion of the same polymers obtained by adiabatic, high-pressure, oxygen bomb calorimetry [41 and 49]. The excellent agreement between PCFC and oxygen bomb calorimetry confirms complete (100%) combustion of typical polymer pyrolysis products in 10 seconds at 900°C in excess oxygen.

Table 2. Net Heats of Combustion of Noncharring Polymer Pyrolyzates by PCFC Compared to Oxygen Bomb Calorimeter Values

Polymer	ASTM D 2015 (kJ/g)	PCFC (kJ/g)	Percent Relative Deviation
Polyethylene	43.3	43.5 ±0.1	0.5
Polystyrene	39.8	39.4 ±0.5	-1.0
Polymethylmethacrylate	24.9	25.0 ±0.1	0.4
Polyoxymethylene	15.9	16.0 ±0.1	0.6

4.3 PYROLYSIS-COMBUSTION FLOW CALORIMETRY.

Figure 9 shows experimental data for the normalized heat release rate Q/β versus temperature for polyoxymethylene (POM), PMMA, polyvinylchloride (PVC), polyethyleneterephthalate (PET), polyamide 66 (PA66), acrylonitrile-butadlene-styrene (ABS), PP, polyvinylidene fluoride (PVDF), PE, fluorinated ethylene-propylene (FEP), polyetherimide (PEI), polyphenylenesulfide (PPS), and polycarbonate (PC) measured by PCFC at a heating rate of 1 K/s using a combustor residence time of 10 seconds at 900°C. The data in figure 9, which is sorted from front to back by the maximum mass loss rate temperature T_{max}, shows that η_c (Q_{max}/β) varies widely in magnitude and temperature for common polymers.

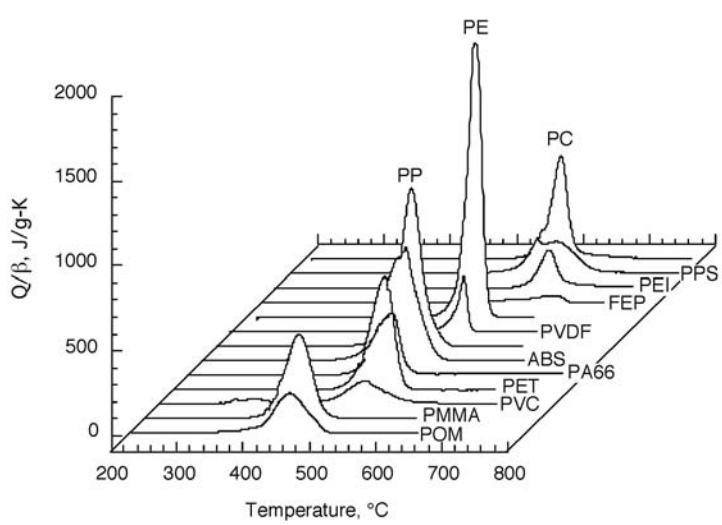

Figure 9. Heat Release Rate Histories of Common Polymers in PCFC

Figure 10 is a plot of the maximum specific HRR Q_{max} versus heating rate for milligram samples of PE, polystyrene (PS), PA66, PMMA, polybutyleneterephthalate/PBT, PET, polyphenleneoxide/PPO, PC, POM, and PT. Symbols are experimental data, and solid lines are calculated from equation 16 for typical value a = 0.06 and β_0 = 1 K/s. Slight negative deviation of Q_{max} versus β from proportionality is expected (equation 16) and observed. However, for the range of heating rates encountered in thermal analyses (β = 0.1-1 K/s) and fires (β_s = 1-10 K/s), the maximum deviation of Q_{max} from proportionality to β is less than 14%, i.e., $[\beta_0/\beta]^a = [\beta_s/\beta_0]^a \approx [10/1]^{\pm 0.06} = 1.00 \pm 0.14$ for a reference heating rate β_0 = 1 K/s. The weak dependence of Q_{max}/β on β is illustrated in figure 11, which shows these data for PE, high-impact polystyrene (HIPS), PMMA, POM, and FEP. Symbols are experimental data, and solid lines are calculated from equation 17 for β_0 = 1 K/s.

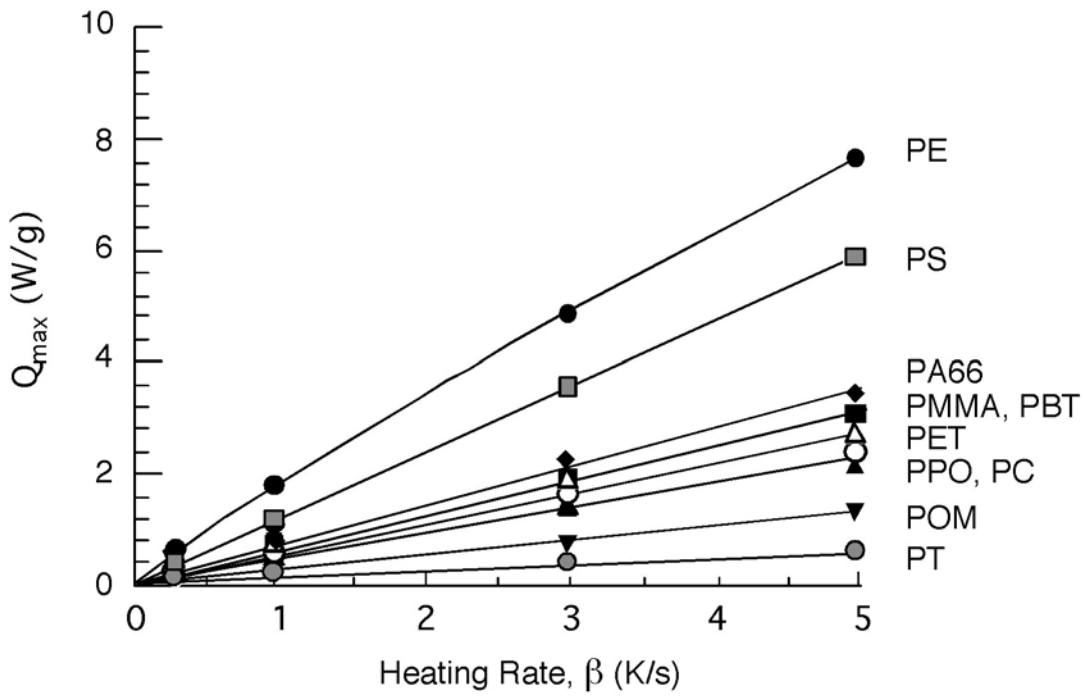

Figure 10. Maximum Specific HRR Q_{max} Versus Heating Rate β in PCFC For 1-mg Samples of PE, PS, PA66, PMMA, PBT, PPO, PC, POM, and PT (Symbols are experimental data. Solid lines are equation 16 with A = 0.06, β_0 = 1 K/s.)

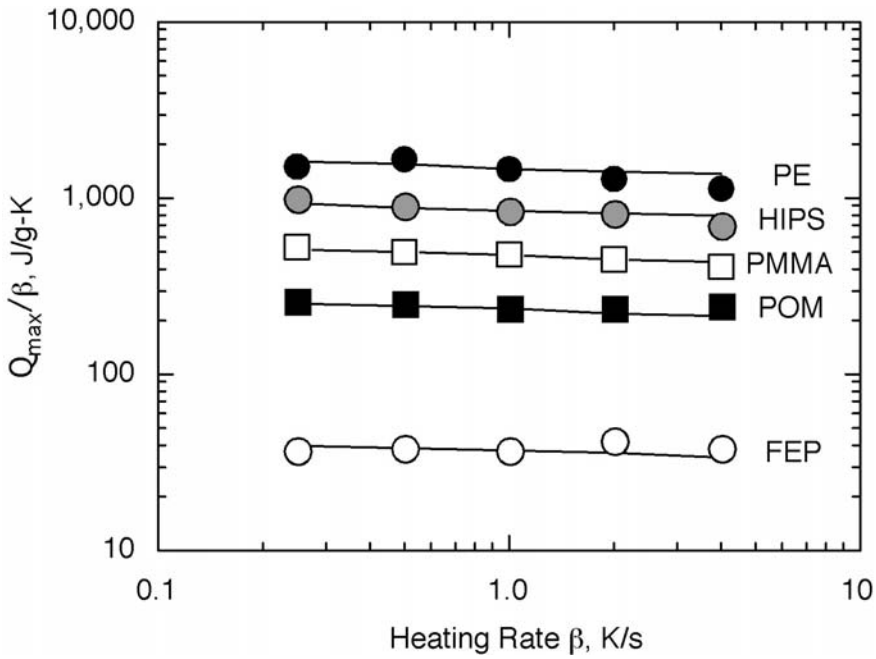

Figure 11. Q_{max}/β Versus β for PE, HIPS, PMMA, POM, and FEP (Symbols are experimental data. Solid lines are equation 17a.)

The repeatability (intralaboratory variation) of measurements made in the laboratory in the apparatus of figure 3 is indicated by the data in table 3, which lists mean values and one standard deviation for triplicate determinations of heat release capacity η_c, total heat released by combustion of volatile fuel h_c^0, char yield μ, and heat release temperature T_{max} of the 14 commercial polymers whose HRR histories are shown in figure 9. Repeatability estimated from the average coefficient of variation for the data in table 3 is better than 5% (i.e., the average relative deviation from the mean is less than 5%). The reproducibility (interlaboratory variation) of measurements for these same polymers obtained using the apparatus of figure 3 is about 10%, as demonstrated graphically in figure 12, which is a plot of individual η_c from each of three different laboratories versus the average η_c for the three laboratories.

Table 3. Flammability Parameters η_c, h_c^0, μ, and T_p for PCFC

Polymer	η_c (J/g-K)	h_c^0 (kJ/g)	μ (%)	T_p (°K)
HDPE	1486 ±20	43.5 ±0.1	0.1 ±0.1	504 ±1
PP	1130 ±24	43.2 ±0.2	0.0 ±0.0	483 ±1
HIPS	859 ±4	37.8 ±0.1	2.5 ±0.2	452 ±1
PA66	623 ±34	29.4 ±0.1	1.0 ±0.1	475 ±2
ABS	581 ±14	37.0 ±0.2	6.2 ±0.3	454 ±1

Table 3. Flammability Parameters η_c, h_c^0, μ, and T_p for PCFC (Continued)

Polymer	η_c (J/g-K)	h_c^0 (kJ/g)	μ (%)	T_p (°K)
PC 2	539 ±26	20.4 ±0.2	22.5 ±0.8	547 ±2
PC 1	484 ±13	20.4 ±0.1	23.2 ±0.2	545 ±3
PMMA	475 ±6	24.9 ±0.1	0.0 ±0.0	393 ±2
PET	357 ±16	16.8 ±0.7	12.6 ±1.5	459 ±3
POM	267 ±19	16.2 ±0.0	0.0 ±0.0	398 ±6
PPS	248 ±27	15.7 ±0.1	44.0 ±0.6	535 ±1
PEI	201 ±7	9.3 ±0.2	51.3 ±0.3	565 ±1
PVC	129 ±3	10.8 ±0.2	18.8 ±0.1	467 ±4
FEP	57 ±1	4.1 ±0.0	0.0 ±0.0	589 ±1

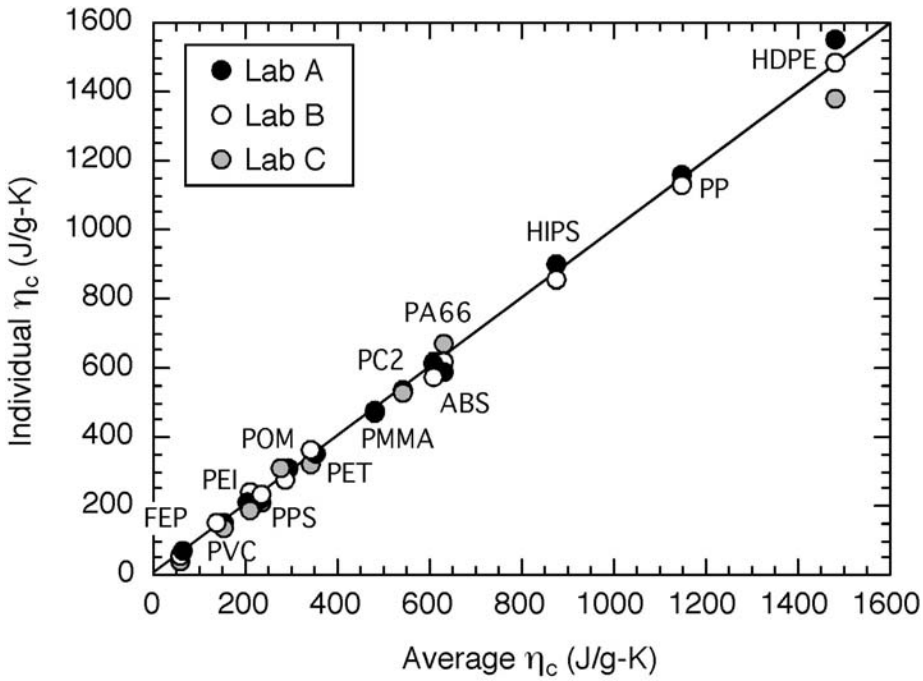

Figure 12. Comparison of Individual and Average Heat Release Capacities From Three Different Laboratories for the 14 Polymers in Table 3

To validate the PCFC method, the heat release capacities of 15 polymers measured by PCFC were compared to those measured for the same samples using a TGA coupled to a gas chromatograph (GC) and mass spectrometer (MS) to determine the fuel species [62-64]. In the TGA-GC/MS method of determining η_c, the thermal decomposition products at maximum mass loss rate are sampled, separated, and analyzed by GC/MS and the resulting data used to compute the heat of complete combustion of the fuel gases $h_{c,v}^0$ from their known or calculated heats of combustion and relative abundance (mass fraction). The heat of combustion so determined is

multiplied by the maximum value of the fractional mass loss rate measured in the TGA at a constant heating rate (e.g., 10 K/min) to obtain the heat release capacity. The heat release capacities normalized to β = 1 K/s measured by PCFC and TGA-GC/MS on samples of the same polymer are plotted on the ordinate and abscissa, respectively, in figure 13. The proximity of the data to the equivalence line indicates an accuracy of about ±16% for η_c obtained by PCFC versus TGA-GC/MS, which is comparable to the experimental uncertainty of the TGA-GC/MS method.

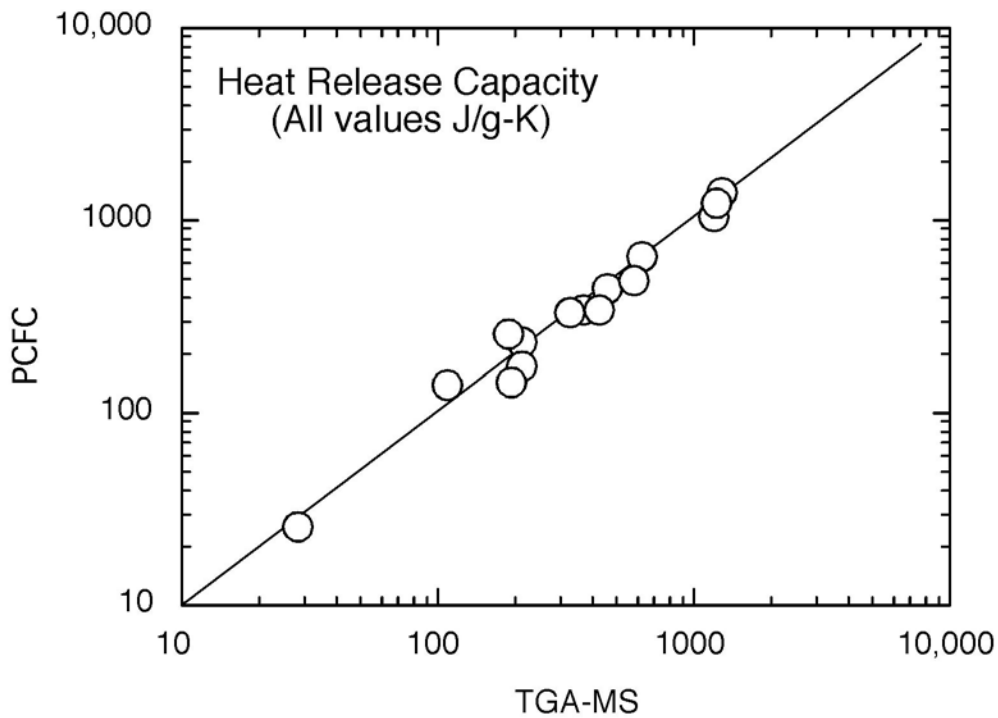

Figure 13. Comparison of Heat Release Capacities Obtained by PCFC at β = 260 K/min and TGA-GC/MS at β = 10 K/min

Figure 14 is a plot of HRR capacity η_c versus $h_c^0/\Delta T_p$ for polymers and commercial plastics that gave a single HRR peak centered at Q_{max} with ΔT_p, the pyrolysis temperature interval at Q_{max}/e. Excellent correlation is observed between heat release capacities obtained by the peak height and peak area methods as per equation 18.

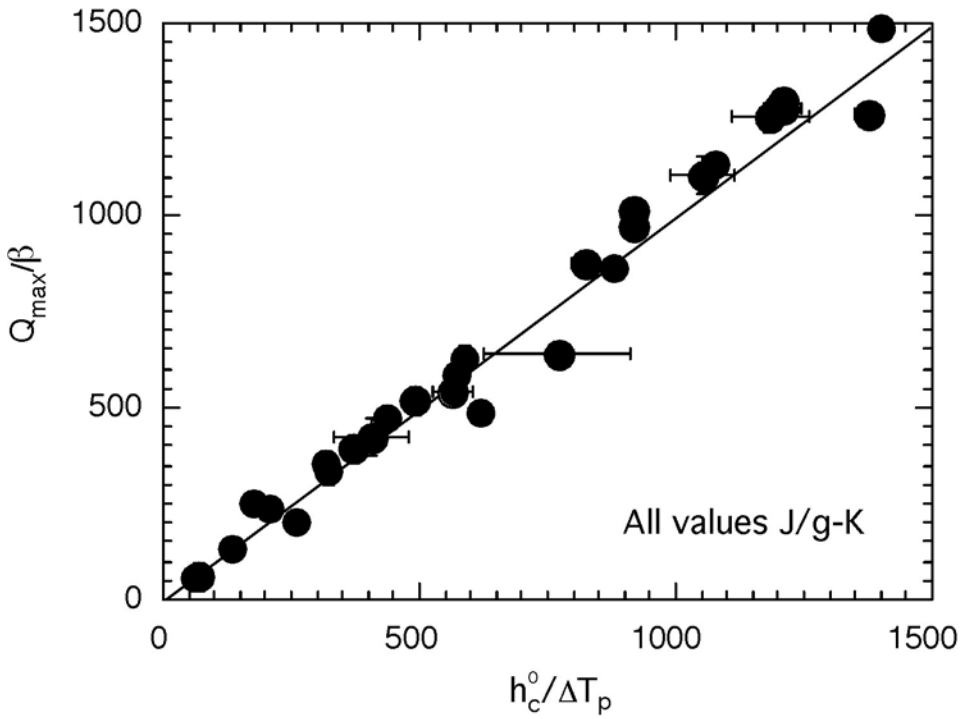

Figure 14. Peak Height Versus Peak Area Method of Calculating the Heat Release Capacity

Experimental data for thermal oxidation of the pyrolysis gases evolved from PC in the TGA at a heating rate β = 20 K/min is shown in figure 15. Residual mass plotted on the right ordinate shows that thermal decomposition begins at about 450°C, and that 24% of the original mass is left as char at the end of the experiment (700°C). The heat of combustion of the thermal decomposition products is obtained by dividing the specific HRR Q(t) by the specific mass loss rate ($m_0^{-1}dm/dt$) at each time t during the test. Figure 15 shows that $h_{c,v}^0$ so obtained ranges from 20-25 kJ/g for the primary decomposition step at 535° ±25°C that generates monomer fragments (phenol, bisphenol, diphenylcarbonate) and a solid primary char [5, 15, and 65]. The primary char decomposes in a second step to a carbon-rich solid over a broad temperature range with the evolution of methane gas [65], which is consistent with the data in figure 15 showing that the heat of combustion of the gases evolved between 550°-700°C, is on the order of methane ($h_{c,v}^0$= 50 kJ/g).

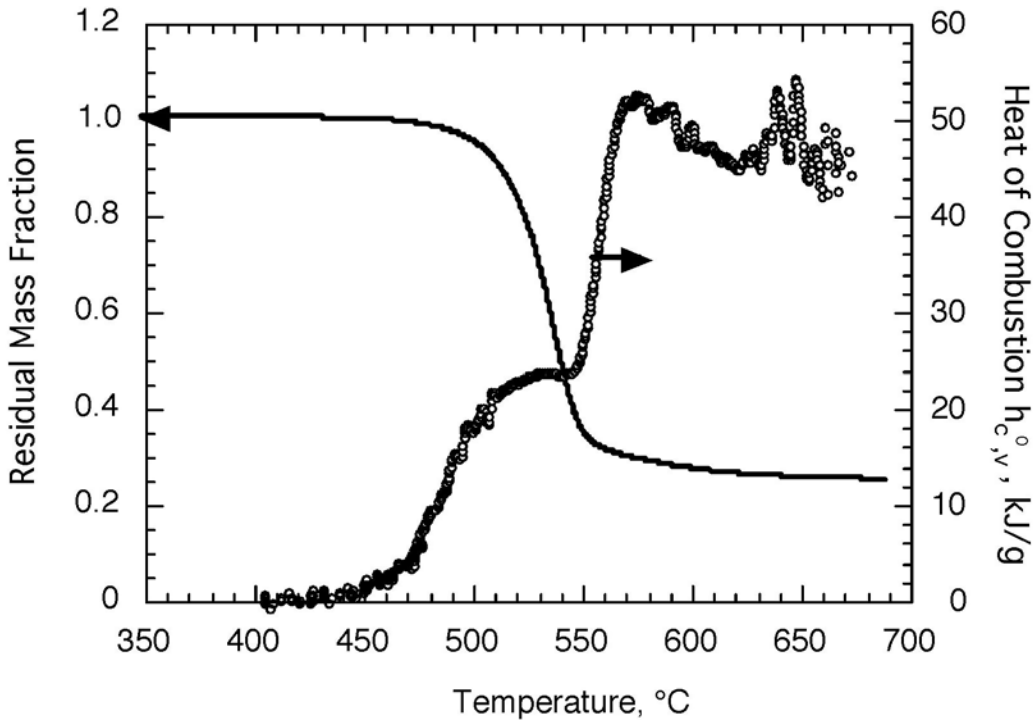

Figure 15. Residual Mass and Heat of Combustion of Pyrolysis Gases Versus Temperature for Test of Polycarbonate in TGA at β = 20 K/min

4.4 OXIDATIVE PYROLYSIS-COMBUSTION FLOW CALORIMETRY.

Figure 16 shows experimental data from oxidative pyrolysis-combustion flow calorimetry (oPCFC) in the apparatus of figure 3 for a 1-mg sample of polycarbonate at β = 5 K/s. Oxidation of the sample gases in the combustor and the delayed oxidation of the solid char in the pyrolyzer during an air purge are shown as separate processes. The area under the Q(t) versus time curve is the net heat of complete combustion of polycarbonate, h_c^o = 29.1 kJ/g in this case. Table 4 compares data for the net heat of combustion of several polymers obtained by oxygen bomb calorimetry [42 and 43] and oPCFC. The accuracy of the oPCFC method, characterized by the average relative deviation of its results from the corresponding oxygen bomb calorimetry measurements, is about 3%.

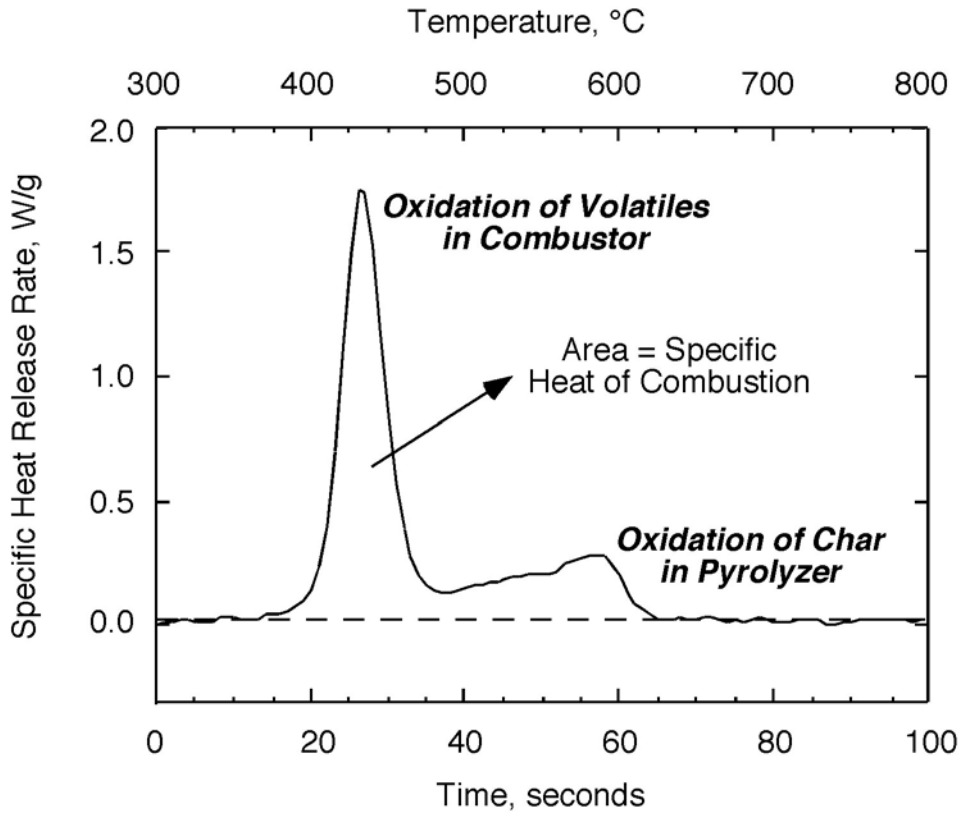

Figure 16. Specific HRR of Polycarbonate Versus Time and Temperature Obtained by oPCFC (Oxidation of gases in combustor and solid char in pyrolyzer are shown as separate processes.)

Table 4. Net Heat of Combustion of Charring ($\mu \neq 0$) and Noncharring ($\mu = 0$) Polymers Obtained by Oxygen Bomb Calorimetry and Oxidative Pyrolysis-Combustion Flow Calorimetry (oPCFC)

Polymer (μ, kg/kg)	ASTM D 2015 (MJ/kg)	oPCFC (MJ/kg)	Relative Deviation (%)
Polyethylene (0)	43.3	43.5	0.5
Polystyrene (0)	39.8	39.4	-1.0
Polymethylmethacrylate (0)	24.9	25.0	0.4
Polyoxymethylene (0)	15.9	16.0	0.6
Polybutyleneterephthalate (0.02)	26.7	26.3	-1.5
Polyethyleneterephthalate (0.13)	21.8	23.2	6.4
Polycarbonate (0.23)	29.8	29.1	-2.3
Polyaramide fiber (0.36)	27.8	28.1	1.1
Polyetheretherketone (0.47)	30.2	30.9	2.3
Phenolic Triazine (0.67)	29.8	29.5	-1.0

4.5 CORRELATION OF PCFC DATA WITH FLAMMABILITY.

4.5.1 Ignitability.

The critical heat flux (CHF) for sustained ignition determines the ease with which a material becomes involved in a fire and is therefore an important fire property [66]. For piloted ignition, CHF $\approx \sigma T_{ign}^4$, where $\sigma = 5.7 \times 10^{-8}$ W/m^2-K^4, is the Boltzmann radiation constant and T_{ign} is the ignition temperature of the material [66]. For hydrocarbon polymers $T_{ign} \approx T_{max}$ and the CHF for sustained, piloted ignition estimated from PCFC data is [25 and 26]

$$\mathrm{CHF} \approx \sigma T_{max}^4 \tag{31}$$

Table 5 lists the average T_{max} for 14 polymers obtained from three different laboratories whose η_c data is plotted in figure 6. Also listed in table 3 are the CHF calculated from T_{max} using equation 31 and generic CHF for these polymers [25 and 26]. Reasonable agreement is observed between the CHF estimated from T_{max} and the CHF measured directly for hydrocarbon polymers. For heteroatom (PPS) and halogen-containing (PVC, PVDF, FEP) polymers with low h_c^0, equation 31 underestimates CHF because, for these polymers, $T_{ign} > T_{max}$ [25, 26, and 66] and HRR is a better predictor of sustained ignition [25 and 26].

Table 5. Critical Heat Flux Calculated From T_{max} Compared to Values Measured in a Fire Calorimeter

Polymer	T_{max} (°C)	CHF, kW/m^2	
		Equation 31	Measured [25]
PMMA	401 ±8	11-12	6-23
POM	409 ±10	11-13	13
HIPS	463 ±10	15-17	15
ABS	467 ±12	16-18	9-15
PET	471 ±12	16-18	10-19
PA66	482 ±11	17-19	15-21
PVC	478 ±8	17-18	15-28
PP	493 ±10	18-20	15-16
PE	514 ±10	20-22	15-20
PVDF	510 ±2	21	30-50
PC	556 ±9	25-28	15-20
PPS	551 ±18	24-28	35-38
PEI	576 ±10	28-31	25-40
FEP	600 ±10	31-34	38-50

4.5.2 Fire Response.

The single best parameter characterizing the fire hazard of a polymer is its HRR (W/m^2) in flaming combustion [67]. However, HRR is difficult to quantify in fire calorimeters because the

test results depend on the external heat flux (heating rate), sample thickness, sample orientation, edge conditions, ventilation rate, etc. In contrast, the heat release capacity measured by PCFC using controlled pyrolysis and complete combustion of the fuel gases depends only on the material being tested. The HRR of a solid polymer in flaming combustion is characterized by a heat of gasification L_g and an effective heat of combustion of the fuel gases (HOC), which is related to h_c^0 by the combustion efficiency in the flame, $\chi = HOC/h_c^0$. The driving force for HRR is the difference between the heat influx from the flame (q''_{flame}) and any external sources (q''_{ext}) and the heat losses from the surface due to reradiation q''_{loss}.

$$HRR = \chi \frac{h_c^0}{L_g}(q''_{flame} - q''_{loss} + q''_{ext}) \tag{32}$$

Defining a dimensionless heat release parameter (HRP) for flaming combustion, $HRP = \chi\, h_c^0/L_g$ and a limiting HRR at zero external heat flux, $HRR_0 = HRP\,(q''_{flame} - q''_{loss})$, the HRR in flaming combustion can be written in linear form [25 and 26] with respect to the independent variable q''_{ext}

$$HRR = HRR_0 + HRP\, q''_{ext} \tag{33}$$

With equation 18, the HRP becomes

$$HRP \equiv \chi \frac{h_c^0}{L_g} = \chi \frac{h_c^0/\Delta T_{p,0}}{L_g/\Delta T_{p,0}} = \frac{\eta_c}{\eta_g} \tag{34}$$

where $\eta_g = L_g/\chi\Delta T_{p,0}$ is a normalizing parameter. From equations 32, 33, and 34, the HRR when $q''_{ext} >> q''_{flame} - q''_{loss}$ is

$$HRR = HRR_0 + HRP\, q''_{ext} \approx HRP\, q''_{ext} = \eta_c \frac{q''_{ext}}{\eta_g} \tag{35}$$

At an external heat flux $q''_{ext} = 50$ kW/m^2, typical of a large fire such that $HRR_0 << HRP\, q''_{ext}$, equation 35 predicts that for typical polymers having $\eta_g = L_g/\chi\Delta T_{p,0} \approx$ (2 MJ/kg)/((0.8)(50K)) = 50 kJ/kg-K

$$HRR = \frac{q''_{ext}}{\eta_g}\eta_c \approx \frac{50\,kW/m^2}{50\,kJ/kg-K}\eta_c = \quad 1\,\frac{kg-K}{m^2-s}\ \eta_c$$

In other words, the HRR in flaming combustion at large external heat flux should be roughly proportional to η_c with slope 1 kg-K/m^2-s at $q''_{ext} = 50$ kW/m^2. Figure 17 is a plot of the peak HRR in flaming combustion measured in a fire calorimeter at $q''_{ext} = 50$ kW/m^2 according to a standard method [47] versus η_c measured in the PCFC for the same or similar polymers. The solid line through the data has the expected slope 1 kg-K/m^2-s and describes the trend reasonably well, considering it represents an average value of η_g.

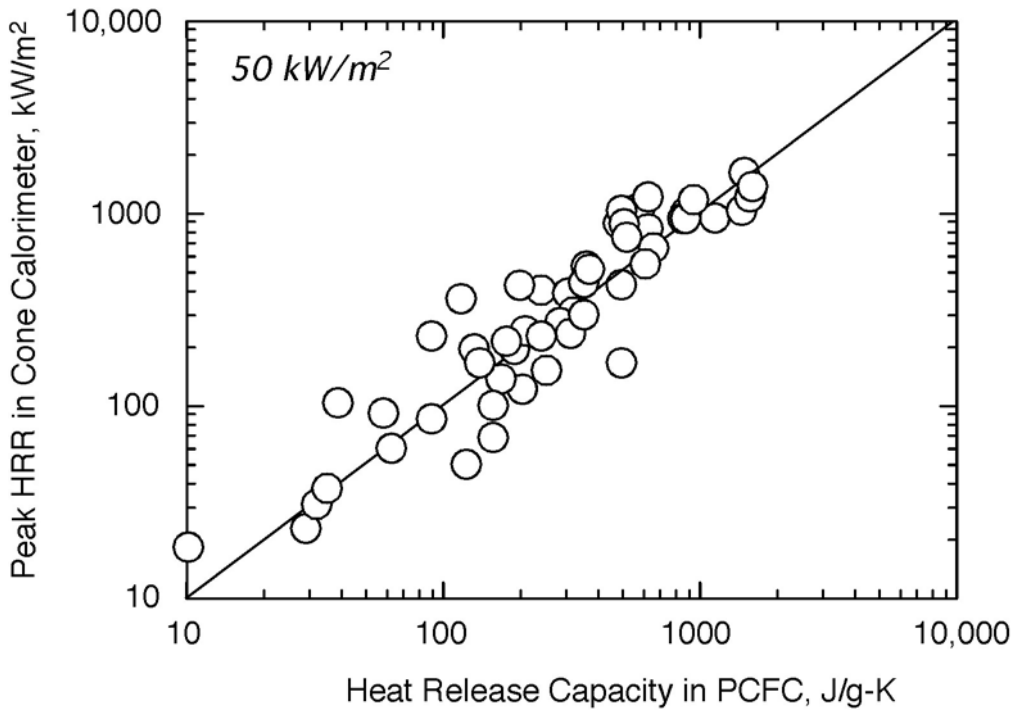

Figure 17. Peak HRR in Cone Calorimeter at 50 kW/m^2 External Flux Versus Heat Release Capacity in PCFC

Figure 18 is a plot of the maximum/peak value of the HRR measured in an OSU fire calorimeter that operates on the sensible enthalpy method [56] versus the heat release capacity η_c of the material. The horizontal dashed line at HRR = 65 kW/m^2 is the maximum HRR value allowed during the standard 5-minute HRR test [56] by Title 14 Code of Federal Regulations Part 25.853(a-1) for large area materials in commercial aircraft cabins. In general, it is seen that peak HRR for these thin materials in the OSU increases with η_c, and the data is roughly approximated (R = 0.64) by a power law, HRR (kW/m^2) = $8\eta_c^{1/2}$. The relatively few data in the range of η_c < 100 J/g-K is a consequence of the fact that only fluoroplastics and research polymers exhibit this low level of flammability and the latter are available in limited quantities.

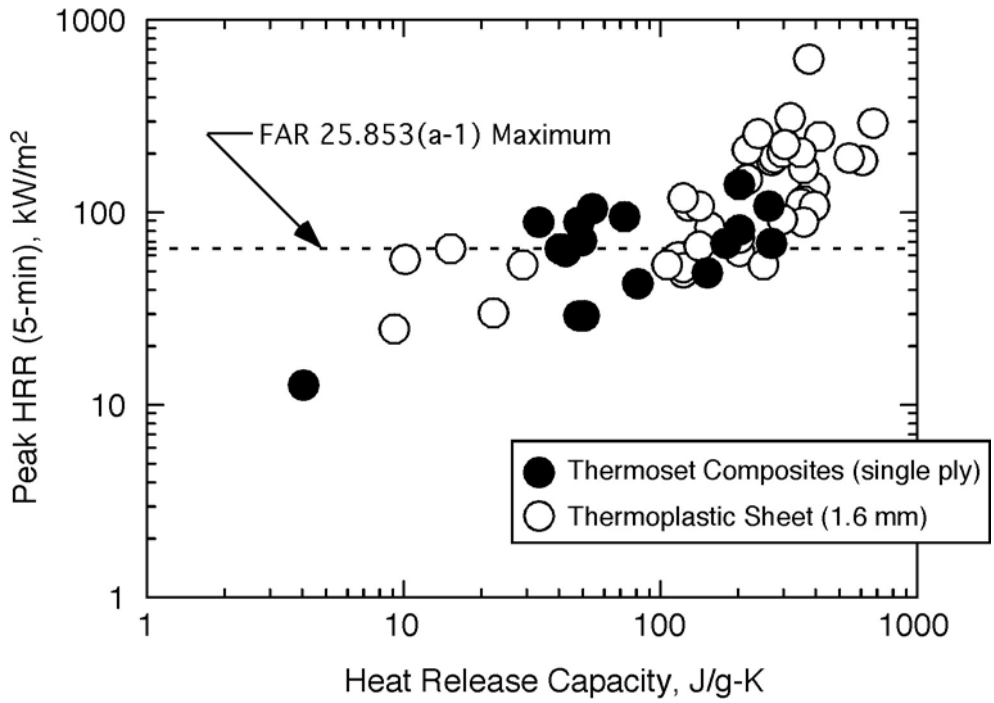

Figure 18. Peak HRR in OSU Versus Heat Release Capacity in PCFC

4.5.3 Flame Resistance.

Flame resistance is an aspect of flammability that relates to the tendency of a thin strip of material to cease burning after brief ignition by a small flame such as a Bunsen burner. The two most popular flame resistance tests are considered here—the limiting oxygen index (LOI) test [57] and the Underwriters Laboratory test for flammability of plastic materials UL 94 [58]. In the latter (UL 94), the time to extinction of the sample flame after removal from a Bunsen burner flame is measured under ambient conditions. At the start of the test, the Bunsen burner is removed and $q''_{ext} = 0$ at $t = 0$. If a minimum (critical) HRR* is required to sustain flaming combustion [25, 26, and 68], then according to equations 33 and 34, flame extinction in the UL test should occur when

$$\mathrm{HRR}(q''_{ext} = 0) = \mathrm{HRR}_0 = \frac{\eta_c}{\eta_g}(q''_{flame} - q''_{loss}) \le \mathrm{HRR}^* \tag{36}$$

For upward burning in air HRR* ≈ 50 kW/m^2 [68] with typical $q''_{flame} \approx 30$ kW/m^2 [69] and $q''_{loss} \approx$ CHF (see table 5), the extinction condition (equation 36) becomes

$$\eta_c \le \frac{\eta_g \mathrm{HRR}^*}{q''_{flame} - q''_{loss}} \approx \frac{(50\,\mathrm{kJ/kg-K})(50\,\mathrm{kW/m^2})}{(30\,\mathrm{kW/m^2} - 17\,\mathrm{kW/m^2})} \approx 200\frac{\mathrm{kJ}}{\mathrm{kg-K}} \tag{37}$$

Figure 19 compares UL 94 vertical test results for polymers to the heat release capacity (η_c) measured in the PCFC for the same or similar compositions spanning a wide range of chemical structure and thermal stability. Figure 19 shows that a transition from sustained burning (no

vertical rating (NR)) to self-extinguishing (V0) occurs at roughly η_c = 200 J/g-K as predicted by equation 37.

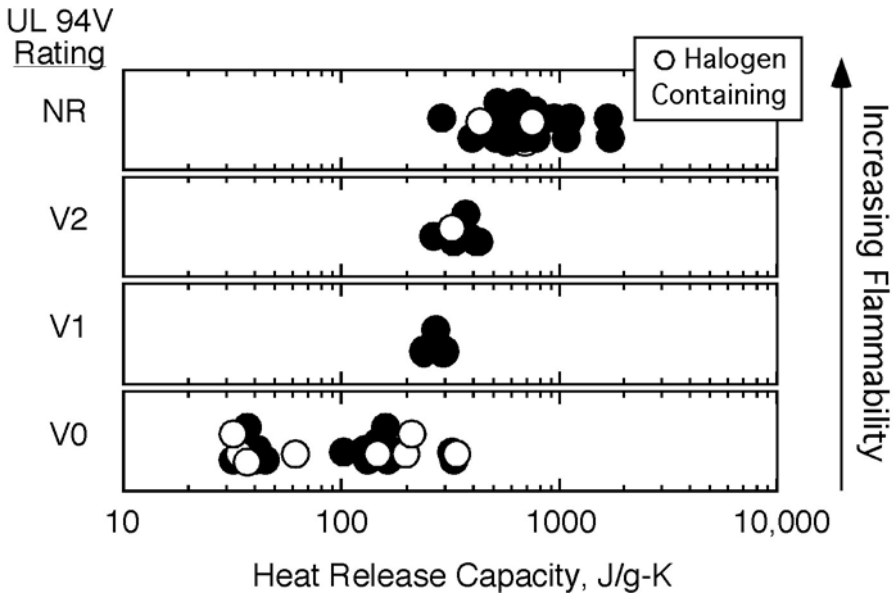

Figure 19. UL 94 V Rating Versus Heat Release Capacity of Polymers
(NR = No rating in vertical test)

In the LOI test, the same initial conditions apply (i.e., q''_{ext} = 0 at t = 0), but the oxygen concentration $[O_2]$ in the test chamber is adjusted until flame extinction occurs. According to Tewarson [69], $q''_{flame} \propto [O_2] = a[O_2]$, equation 36 predicts that flame extinction occurs in the LOI test when

$$\eta_c \le \frac{\eta_g \, HRR^*}{q''_{flame} - q''_{loss}} = \frac{\eta_g \, HRR^*}{a[O_2] - q''_{loss}} \tag{38}$$

or

$$LOI = [O_2]^* = \frac{q''_{loss}}{a} + \frac{\eta_g \, HRR^* / a}{\eta_c} \tag{39}$$

Surface heat losses are of the order (see table 5) $q''_{loss} = \sigma T_{ign}^4 \approx 17$ kW/m^2, and the critical heat release for downward burning in the LOI test is HRR* ≈ 100 kW/m^2 [68]. Empirically, it is found that a = 1.40 kW/m^2-%$[O_2]$, so the oxygen concentration at extinction $[O_2]^*$ = LOI from equation 39 is

$$\mathrm{LOI} = \frac{17\,\mathrm{kW/m^2}}{1.4\,\mathrm{kW/m^2} - \%[\mathrm{O_2}]} + \frac{(50\mathrm{kJ/kg-K})(100\mathrm{kW/m^2})/(1.4\,\mathrm{kW/m^2} - \%[\mathrm{O_2}])}{\eta_c}$$

$$= 12\% + \frac{4000}{\eta_c}(\%) \tag{40}$$

Figure 20 is a plot of LOI versus η_c for polymers of the same or similar composition. The solid line through the data is equation 40, which provides a reasonable correlation of the data for both hydrocarbon and halogen-containing polymers.

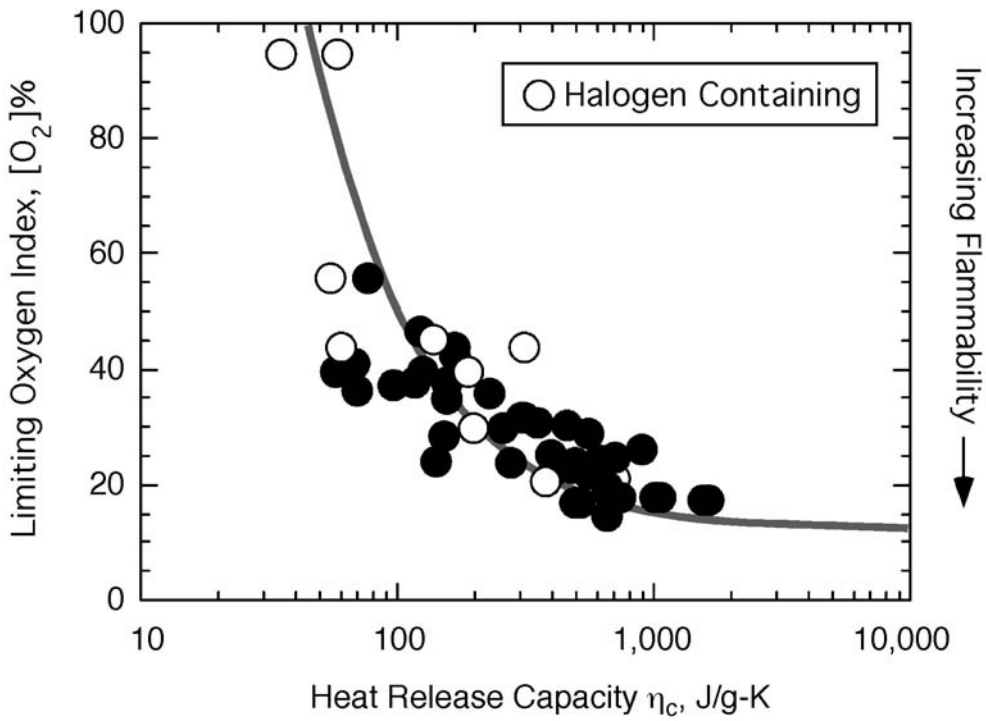

Figure 20. Limiting Oxygen Index Versus Heat Release Capacity of Polymers
(Solid line through data is equation 40.)

Equations 36-40 and figures 19 and 20 show that η_c is a good predictor of flame test results because self-extinction in these tests is a critical phenomenon that occurs over a narrow range of HRR (50-100 kW/m^2) and, consequently, a particular value of η_c [25 and 26].

- $\eta_c \geq 400$ J/g-K; No NR in the UL 94 vertical burn test and LOI < 25.
- η_c = 200-400 J/g-K; Self-extinguishing in UL test (V2/V1) and LOI = 25-30.
- η_c = 100-200 J/g-K; Self-extinguishing in UL test (V0/5V) and LOI = 30-40.
- $\eta_c \leq 100$ J/g-K; No ignition (no after-flame in UL test) and LOI > 40. These materials usually pass strict FAA requirements for the HRR of materials used in commercial aircraft cabins [70].

5. CONCLUSIONS.

A thermal analysis method for laboratory determination of flammability parameters of materials using milligram-sized samples was presented. The method separately reproduces the condensed phase (pyrolysis) and gas phase (combustion) processes of flaming combustion in a single test and forces them to completion. Decoupling the pyrolysis and combustion processes in this way isolates the chemistry of the condensed phase from the test environment and provides the maximum potential (capacity) of the material to release heat in fires. The heat release capacity so measured is related to flame and fire test results using a simple burning model that, like the pyrolsis-combustion flow calorimetry test, does not capture physical phenomenon, such as melting, dripping, and swelling, that can have a real and varied effect on fire behavior.

6. REFERENCES.

1. Pearce, E.M., Khanna, Y.P., and Raucher, D., "Thermal Analysis of Polymer Flammability," in *Thermal Characterization of Polymeric Materials*, E.A. Turi, ed., Academic Press, Orlando, FL, 1981, pp. 793-843.

2. Hassel, H.L., "Evaluation of Polymer Flammability by Thermal Analysis," *American Laboratory*, 9(1), 1977, pp. 35-37.

3. Aseeva, R.A. and Grygorovskaya, V.A., "Thermal Properties and Flammability of Polyarylenes and Their Modifying Products," *Polymer Degradation & Stability*, 64, 1999, pp. 457-463.

4. Mark, H.F., Atlas, S.M., Shalaby, S.W., and Pearce, E.M., "Combustion of Polymers and its Relatardation," in *Flame Retardancy of Polymeric Materials*, M. Lewin, S.M. Atlas, and E.M. Pearch, eds., Plenum Press, NY, 1975, pp. 1-17.

5. Cullis, C.F. and Hirschler, M.M., "The Signficance of Thermoanalytical Measurements in the Assessment of Polymer Flammability," *Polymer*, 24(7), 1983, pp. 834-840.

6. Weisner, E., "Study of the Flammability of Polymers by Thermal Analysis," *Chemicke Vlakna*, 26(3-4), 1976, pp. 146-150.

7. Mickelson, R.W., "Using Thermal Analysis to Confirm the Flammability Behavior of a Polymer," *Proceedings of the American Chemical Society Meeting*, 33(1), 1973, pp. 485-489.

8. Carroll-Porczynski, C.Z., "Applications of Simultaneous DTA/TGA and DTA/MS Analysis for Predicting the Flammability of Composite Textile Fabrics and Polymers," *Composites*, 4(1), 1973, pp. 9-15.

9. Cullis, C.F., "The Role of Pyrolysis in Polymer Combustion and Flame Retardance," *Journal of Analytical and Applied Pyrolysis*, 11, 1987, pp. 451-463.

10. Balog, K., Kosik, S., Kosik, M., Reiser, V., and Simek, I., "Application of Thermal Analysis Procedures to the Combustion and Flammability of Some Polymers," *Thermochimica Acta*, 93, 1985, pp. 167-170.

11. Simon, J., Androsits, B., and Kozma, T., "Study of the Process of Flame Retardation by Thermal Analysis," *Magyar Kemikusok Lapja*, 36(10), 1981, pp. 510-514.

12. van Krevelen, D.W., "Some Basic Aspects of Flame Resistance of Polymeric Materials," *Polymer*, 16, 1975, pp. 615-620.

13. Carty, P. and White, W., "The Importance of Char Forming Reactions in Thermoplastic Polymers," *Fire & Materials*, 18, 1994, pp. 151-166.

14. Murashko, E.A., Levchik, G.F., Levchik, S.V., Bright, D.A., and Dashevsky, S., "Fire Retardant Action of Resorcinol Bis(Diphenyl Phosphate) in a PC/ABS Blend. I. Combustion Performance and Thermal Decomposition Behavior," *Journal of Fire Sciences*, 16, 1998, pp. 278-295.

15. Hirschler, M.M., "Chemical Aspects of Thermal Decomposition of Polymeric Materials," in *Fire Retardancy of Polymeric Materials*, A.F. Grand and C.A. Wilkie, eds., Marcel Dekker, New York, 2000, pp. 28-75.

16. Gracik, T.D. and Long, G.L., "Prediction of Thermoplastic Flammability by Thermo-gravimetry," *Thermochimica Acta*, 212, 1992, pp. 163-170.

17. Kashiwagi, T., "Polymer Combustion and Flammability-Role of the Condensed Phase," *Proceedings of the 25th Symposium (International) on Combustion*, The Combustion Institute, 1994, pp. 1423-1437.

18. Lyon, R.E., "Solid-State Thermochemistry of Flaming Combustion," in *Fire Retardancy of Polymeric Materials*, A.F Grand and C.A. Wilkie, eds., Marcel Dekker, Inc., New York, NY, 2000, pp. 391-447.

19. Lyon, R.E., "Heat Release Kinetics," *Fire and Materials*, 24, 2000, pp. 179-186.

20. Lyon, R.E., "Heat Release Capacity," *Proceedings of the Fire & Materials Conference*, San Francisco, CA, January 22-24, 2001.

21. Lyon, R.E., "A New Method for Measuring Polymer Flammability," *Flame Retardants 2002*, London, England, February 5-6, 2002.

22. Lyon, R.E., and Walters, R.N., "Heat Release Capacity: A Molecular Level Fire Response Parameter," *Proceedings of the 7th International Symposium on Fire Safety Science*, Intl. Assoc. for Fire Safety Science, Worcester, MA, 2003, pp. 1167-1168.

23. Walters, R.N. and Lyon, R.E., "Molar Group Contributions to Polymer Flammability," *Journal of Applied Polymer Science*, 87, 2003, pp. 548-563.

24. Zhang, H., "Fire Safe Polymers and Polymer Composites," FAA report DOT/FAA/AR-04/11, September 2004.

25. Lyon, R.E., "Plastics and Rubber," in *Handbook of Building Materials for Fire Protection*, C. A. Harper, ed., McGraw-Hill, New York, NY, Chapter 3, 2004, pp. 3.1-3.51.

26. Lyon, R.E. and Janssens, M., "Polymer Flammability," *Encyclopedia of Polymer Science & Engineering (on-line edition)*, John Wiley & Sons, New York, NY, October 2005.

27. Lyon, R.E., "Pyrolysis Kinetics of Char Forming Polymers," *Polymer Degradation and Stability*, 61(2), 1998, pp. 201-210.

28. Moghtaderi, B., Novozhilov, V., Fletcher, D., and Kent, J.H., "An Integral Model for the Transient Pyrolysis of Solid Materials," *Fire and Materials*, 21, 1997, pp. 7-16.

29. Quintiere, J. and Iqbal, N., "An Approximate Integral Model for the Burning Rate of a Thermoplastic-Like Material," *Fire and Materials*, 18, 1994, pp. 89-98.

30. Chen, Y., Delichatsios, M.A., and Motevalli, V., "Material Pyrolysis Properties, Part I: An Integral Model for One-Dimensional Transient Pyrolysis of Charring and Non-Charring Materials," *Combustion Science & Technology*, 88, 1993, pp. 309-328.

31. Staggs, J.E.J. and Whiteley, R.H., "Modeling the Combustion of Solid-Phase Fuels in Cone Calorimeter Experiments," *Fire and Materials*, 23, 1999, pp. 63-69.

32. Staggs, J.E.J. and Nelson, M.I., "A Critical Mass Flux Model for the Flammability of Thermoplastics," *Combustion Theory and Modeling*, 5, 2001, pp. 399-427.

33. Staggs, J.E.J., "Modeling Thermal Degradation of Polymers Using Single-Step First-Order Kinetics," *Fire Safety Journal*, 32, 1999, pp. 17-34.

34. Bucsi, A. and Rychly, J., "A Theoretical Approach to Understanding the Connection Between Ignitability and Flammability Parameters of Organic Polymers," *Polymer Degradation and Stability*, 38, 1992, pp. 33-40.

35. Lyon, R.E. "An Integral Method of Nonisothermal Kinetic Analysis," *Thermochimica Acta,* 297, 1997, pp. 117-124.

36. Grassie, N. and Scotney, A., "Activation Energies for Thermal Degradation of Polymers," in *Polymer Handbook,* 2nd Edition, J. Brandrup and H. Immergut, eds., Wiley-Interscience, NY, pp. II, 1975, pp. 467-471.

37. Van Krevelen, D.W., *Properties of Polymers*, Elsevier, Amsterdam, 1990, pp. 627-653.

38. Bicerano, J., *Prediction of Polymer Properties*, 2nd Edition, Marcel Dekker, New York, NY, 1996.

39. ASTM Standard E 2008, Test Method for Volatility Rate by Thermogravimetry, ASTM International, West Conshohocken, PA.

40. ASTM Standard E 1641, Test Method for Decomposition Kinetics by Thermogravimetry, ASTM International, West Conshohocken, PA.

41. Walters, R.N., "Molar Group Contributions to the Heat of Combustion," *Fire and Materials*, 26, 2002, pp. 131-145.

42. Babrauskas, V., "Heat of Combustion and Potential Heat," V. Babrauskas, S.J. Grayson, eds., *Heat Release in Fires*, Elsevier, (Chapter 8) New York, 1992, pp. 207–223.

43. Thornton, W.M., "The Relation of Oxygen to the Heat of Combustion of Organic Compounds," *Philosophical Magazine,* 33, 1917, p. 196.

44. Huggett, C., "Estimation of Rate of Heat Release by Means of Oxygen Consumption Measurements," *Fire and Materials,* 4(2), 1980, p. 61.

45. Janssens, M.L., "Measuring Heat Release by Oxygen Consumption," *Fire Technology*, 27, 1991, p. 234.

46. Janssens, M. and Parker, W.J., "Oxygen Consumption Calorimetry," V. Babrauskas, S.J. Grayson, eds., *Heat Release in Fires* (Chapter 3), Elsevier, New York, 1992, pp. 31-59.

47. ASTM Standard 1354, Test Method for Heat and Visible Smoke Release Rates for Materials and Products Using and Oxygen Consumption Calorimeter, ASTM International, West Conshohocken, PA.

48. ASTM Standared E 2058, Test Method for Measurement of Synthetic Polymer Material Flammability Using a Fire Propagation Apparatus (FPA), ASTM International, West Conshohocken, PA.

49. Walters, R.N., Hackett, S.M., and Lyon, R.E., "Heats of Combustion of High Temperature Polymers," *Fire and Materials*, 24, 2000, pp. 245-252.

50. ASTM Standard D 2015, Test Method for Gross Calorific Value of Coal and Coke by the Adiabatic Bomb Calorimeter, ASTM International, West Conshohocken, PA.

51. Lyon, R.E. and Walters, R.N., "A Pyrolysis-Combustion Flow Calorimeter for the Study of Polymer Heat Release Rate," *Proc. 9th Annual BCC Conference on Flame Retardancy of Polymeric Materials*, Stamford, CT, June 1-3, 1998.

52. Microscale Combustion Calorimeter, U.S. Patent 5,981,290, November 9, 1999.

53. Lyon, R.E. and Walters, R.N., "A Microscale Combustion Calorimeter," FAA report DOT/FAA/AR-01/117, February 2002.

54. Heat Release Rate Calorimeter For Milligram Samples, U.S. Patent 6,464,391, October 15, 2002.

55. Lyon, R.E. and Walters, R.N., "Pyrolysis Combustion Flow Calorimetry," *Journal of Analytical and Applied Pyrolysis*, 71(1), 2004, pp. 27-46.

56. Heat Release Rate Test for Cabin Materials as per Federal Aviation Regulation 25.853, "Aircraft Materials Fire Test Handbook," Section 5, final report DOT/FAA/AR-00/12, April 2000.

57. ASTM Standard D 2863, Test Method for Measuring the Minimum Oxygen Concentration to Support Candle-Like Combustion of Plastics (Oxygen Index), ASTM International, West Conshohocken, PA.

58. Flammability of Plastic Materials, UL 94, Section 3 (Vertical: V-0/1/2), Underwriters Laboratories, Northbrook, IL, 1991.

59. Heffington, W.M., Parks, G.E., Sulzmann, K.G.P., and Penner, S.S., "Studies of Methane Oxidation Kinetics," *Sixteenth Symposium (International) on Combustion*, The Combustion Institute, 1976, pp. 997-1010.

60. Reshetnikov, S.M. and Reshetnikov, I.S., "Oxidation Kinetic of Volatile Polymer Degradation Products," *Polymer Degradation and Stability*, 64, 1999, pp. 379-385.

61. Babrauskas, V., Parker, W.J., Mulholland, G., and Twilley, W.H., "The Phi Meter: A Simple, Fuel-Independent Instrument for Monitoring Combustion Equivalence Ratio," *Review of Scientific Instruments*, 65(7), 1994, pp. 2367-2375.

62. Schoemann, A., Westmoreland, P.R., Zhang, H., Farris, R.J., Walters, R.N., and Lyon, R.E., "A Pyrolysis/GC-MS Method for Characterizing Flammability and Thermal Decomposition of Polymers," *Proc. 4th Joint Meeting of the U.S. Sections of the Combustion Institute*, Philadelphia, PA, March 21-23, 2005.

63. Westmoreland, P.R., Inguilzian, T., and Rotem, K., "Flammability Kinetics From TGA/DSC/GCMS, Microcalorimetry and Computational Quantum Chemistry," *Thermochmica Acta* 67, 2001, pp. 401-405.

64. Inguilizian, T.V., "Correlating Polymer Flammability Using Measured Pyrolysis Kinetics," Master of Science Thesis, University of Massachusetts, Amherst, January 1999.

65. Factor, A., "Char Formation in Aromatic Engineering Polymers," *Fire and Polymers*, G.L. Nelson, ed., ACS Symposium Series 425, American Chemical Society, Washington, D.C., 1990, pp. 274-287.

66. Babrauskas, V., *Ignition Handbook*, Fire Science Publishers, Issaquah, WA, 2003.

67. Babaruskas, V. and Peacock, R.D., "Heat Release Rate: The Single Most Important Variable in Fire Hazard," *Fire Safety Journal*, 18, 1992, pp. 255-272.

68. Lyon, R.E., "Fire & Flammability," *Fire Risk & Hazard Assessment Research Symposium*, Fire Protection Research Foundation, Baltimore, MD, July 9-11, 2003, pp. 22-32.

69. Tewarson, A., Lee, J.L., and Pion, R.F., "The Influence of Oxygen Concentration on Fuel Parameters for Fire Modeling," *Eighteenth Symposium (International) on Combustion*," The Combustion Institute, Pittsburgh, PA, pp. 563-570, 1981.

70. Walters, R.N. and Lyon, R.E., "Flammability of Automotive Plastics," Presented at the *Society of Automotive Engineers (SAE) World Congress & Exposition*, Detroit, MI, April 3-6, 2006.